



UNIVERSITY OF NAIROBI

**POTENTIAL OF PREDICTING RAINFALL ONSET AND CESSATION
DATES IN KENYA USING TROPOSPHERIC MOISTURE
ACCUMULATION**

JELAGAT VICTORINE

I56/8558/2017

**A DISSERTATION SUBMITTED FOR EXAMINATION IN PARTIAL
FULFILMENT OF THE REQUIREMENTS FOR AWARD OF THE
DEGREE OF MASTERS OF SCIENCE IN METEOROLOGY OF THE
UNIVERSITY OF NAIROBI**

DEPARTMENT OF METEOROLOGY

NOVEMBER 2020

DECLARATION

I declare that this dissertation is my original work and has not been submitted elsewhere for examination, award of a degree or publication. Where other people's work or my own work has been used, this has properly been acknowledged and referenced in accordance with the University of Nairobi's requirements.

Signature -----

Jelagat Victorine

Date

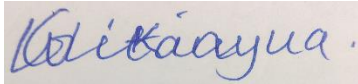
I56/8558/2017

Department of Meteorology

University of Nairobi

This dissertation has been submitted for examination with our approval as the university supervisors:

Signature -----



17/11/2020

Dr. Wilson Gitau

Date

Department of Meteorology

University of Nairobi

P.O Box 30197-00100

Nairobi Kenya

Signature -----

Dr Franklin Opijah

Date

Department of Meteorology

University of Nairobi

P.O Box 30197-00100

Nairobi Kenya

DEDICATION

I dedicate this work to my family and to all with unquenched thirsty of finding solutions and solving societal issues.

ACKNOWLEDGEMENT

I wish to express my gratitude to God the Almighty for His faithfulness and sustenance during my schooling.

I also wish to convey my appreciation to my supervisors Dr, Wilson Gitau and Dr. Franklin Opijah for their regular guidance, suggestions, encouragement and patience. Without your unwavering support this work would not have come to a reality. I also wish to extend my heartfelt gratitude to the University of Nairobi for granting me a scholarship to further my studies. To all the staff and students of the Department of Meteorology, University of Nairobi, you all feel appreciated for your support during my study period.

I extend my sincere credit to all my friends who in one way or another contributed to the success of this work. A special mention goes to; Dr. Emily Bosire who taught me macros and Dr. Bethwel Mutai for his constant push.

To all my family members, your prayers and support have bore fruits. Thank you all for believing in me.

ABSTRACT

Rainfall portrays high variability in space and time in Kenya. The severity of rainfall variability demonstrated as excessively heavy precipitation (floods) or excessively light rainfall (droughts) affects the economy of the country, which largely depends on seasonal rainfall. High variability of intra-seasonal rainfall characteristics such as the start, the end and the length of the season leads to adverse effects on the socio-economic activities in the country.

The main objective of this study was to determine the potential of predicting rainfall onset and cessation dates over Kenya using tropospheric moisture accumulation during the long and short rainfall seasons. Daily rainfall dataset used were Climate Hazards Infrared Precipitation with Stations (CHIRPs) which is a blend of satellite estimates with rain gauge rainfall covering the period 1981-2018 with a resolution of 0.05°; tropospheric daily temperature and relative humidity circulation variables derived from the 5th generation of European Centre for Medium-Range Weather Forecasts Re-Analysis (ERA-5) spanning from 1989-2018 at a resolution 0.25°.

The CHIRPS data was analyzed by means of the scores from the Principal Component Analysis (PCA). Dates of the start and end of seasonal rainfall was determined using the first PCA score (PC1). Accumulated minimum (maximum) values equate to the start (end) date of the rainy season. Clausius Clapeyron, Poisson and specific humidity equations were some of the equations used to determine the equivalent potential temperature and saturation equivalent potential temperature and their anomalies computed in order to assess the moisture supply in the atmosphere. These anomalies were the basis for the determination of the time lags which determined the predicted start and end dates of rainfall.

Over the study region the start date of rains occurred between 15th March to 08th April while the cessation ranged from 20th April to 29th May during the long rainy (MAM) season. Short rainy (OND) season on the other hand recorded onset (cessation) which ranged from 23rd September to 11th November (28th November to 27th December).

Identification of the dates of onset and withdrawal of moisture accumulation were performed using time series plots. The antecedent months were considered, in this case January and February for MAM season and July and August for OND season. The start of moisture build up and withdrawal come early before the exact dates of the seasonal rainfall. The mean start (end)

dates of moisture build up ranged from pentad 3 to pentad 6 (pentad 11 to pentad 15) during the MAM season and pentad 4 to pentad 7 (pentad 14 to pentad 24) during the OND at the 700 hPa level. Using the data at 850 hPa level, the mean start (end) of moisture build up ranged from pentad 4 to pentad 8 (pentad 9 to pentad 17) for the March-April-May season while during the OND season the mean start and end of moisture build up ranged from pentad 41 to pentad 49 and pentad 53 to pentad 69 respectively.

Time lags obtained are the lead time used to obtain the predicted onset and cessation of rainfall. The time lags were added to the pentads of moisture build up and withdrawal to give the onset and cessation of rains prior the start and end of rainfall. It ranged from 7 to 15 (10 to 19) pentads for the onset (cessation) at the 850 hPa, during the MAM season. The 700 hPa level obtained 8 to 15 (5 to 19) pentads for the onset (cessation). Conversely, the OND season recorded 7 to 21 (2 to 11) pentads for the onset (cessation) at the 850 hPa whereas 10 to 22 pentads and 2 to 11 pentads were recorded for the onset and cessation of moisture build up respectively at the 700 hPa level.

Interannual variability of the actual and predicted onset and cessation portrayed non-uniform pattern in the time series. The relationship between actual and predicted onset, and the actual and predicted cessation was insignificant for most stations. Kisumu, Moyale, Voi and Wajir recorded some significant correlation. Kisumu for instance recorded significant relationship with a correlation coefficient of 0.424 (-0.523) between actual and predicted onset (cessation) at 850 hPa level during the October-November-December season. Moyale recorded a correlation coefficient (CC) of 0.401 (-0.372) between the actual and predicted cessation for 850 hPa (700 hPa) level while a CC of -0.375 (1) between the actual and predicted onset (cessation) during the OND season at 850 hPa.

The results of the study show the prospective of utilizing tropospheric moisture variables in predicting rainfall start and end dates over the study domain. The method (PCA method) used in determination of the start and end of rainfall dates in this study should be operational since it is able to detect co-variabilities in station rainfall.

TABLE OF CONTENTS

DECLARATION	ii
DEDICATION	iii
ACKNOWLEDGEMENT	iv
ABSTRACT	v
TABLE OF CONTENTS	vii
LIST OF FIGURES	ix
LIST OF TABLES	xi
ABBREVIATIONS AND ACROYNMS	xii
CHAPTER ONE	1
1.0 INTRODUCTION	1
1.1 Background of the Study	1
1.2 Problem Statement	2
1.3 Objective of the Study	3
1.4 Justification of the Study	3
1.5 Domain of the Study	4
CHAPTER TWO	7
2.0 LITERATURE REVIEW	7
2.1 Studies on onset and cessation based on rainfall	7
2.2 Studies on the onset and cessation of rainfall using tropospheric circulation variables	11
CHAPTER THREE	14
3.1 Data Type and Source	14
3.1.1 Climate Hazards Infrared Precipitation with Stations	14
3.1.2 Temperature and Relative Humidity	15
3.2 Methodology	16
3.2.1 Determination of Onset and Cessation Dates of Rainfall	16
3.2.2 Identification of moisture commencement and withdrawal dates	16
3.2.3 Evaluation of the linkage between rainfall onset and cessation dates, and the moisture build-up and withdrawal of moisture dates	18
CHAPTER FOUR	20

4.0 RESULTS AND DISCUSSIONS	20
4.1 Onset and Cessation dates of Rainfall	20
4.1.1 Interannual Variability of the Dates of Onset and Cessation of Rainfall.....	21
4.1.2 Spatial distribution of the mean start and end dates	25
4.2 Dates of Commencement and Withdrawal of Moisture	27
4.3 Linkage between Rainfall Onset and Cessation dates; and the Start and End dates of Moisture accumulation	30
4.3.1 Correlation analysis.....	40
CHAPTER FIVE	42
5.0 CONCLUSIONS AND RECOMMENDATIONS	42
5.1 CONCLUSIONS	42
5.2 RECOMMENDATIONS.....	43
5.2.1 Recommendation to Climate Services Providers and Policy Makers.....	43
5.2.2 Recommendations to Scientists and Climate Research Institutions	44
5.2.3 Recommendation to Users of Climate Information.....	44
References	45

LIST OF FIGURES

<i>Figure 1: Digital elevation map for Kenya showing physical features. The lakes are in blue and elevations rise from the coast westwards (Omondi, 2015).....</i>	<i>5</i>
<i>Figure 2: Onset (green dot) and cessation (red dot) date of rainfall at (a) Marsabit during MAM season and (b) Dagoretti during OND season for the year 1986</i>	<i>20</i>
<i>Figure 3 : Interannual variability of rainfall onset (blue time series) and cessation (red time series) over Kisumu during MAM season from 1980 to 2018.....</i>	<i>22</i>
<i>Figure 4: Interannual variability of rainfall onset (blue time series) and cessation (red time series) over Marsabit during the MAM season from 1980-2018</i>	<i>22</i>
<i>Figure 5: Interannual variability of rainfall onset (blue time series) and cessation (red time series) over Voi during MAM season from 1980-2018</i>	<i>23</i>
<i>Figure 6: Interannual variability of rainfall onset (blue time series) and cessation (red time series) over Kakamega during the OND season from 1980-2017</i>	<i>24</i>
<i>Figure 7: Interannual variability of rainfall onset (blue time series) and cessation (red time series) over Lamu during the OND season from 1980-2017</i>	<i>25</i>
<i>Figure 8: Interannual variability of rainfall onset (blue time series) and cessation (red time series) over Nakuru during the OND season from 1980-2017.....</i>	<i>25</i>
<i>Figure 9: Spatial distribution of mean onset (a) and cessation (b) dates of rainfall during the MAM season for the period 1981-2018 over Kenya</i>	<i>26</i>
<i>Figure 10 Spatial distribution of mean onset (a) and cessation (b) dates of rainfall during the OND season for the period 1981-2017 over Kenya</i>	<i>27</i>
<i>Figure 11: Pentad series for equivalent potential temperature (blue series) and saturation equivalent potential temperature (red series) anomalies for MAM season during the year 1989 for Dagoretti station at 850 hPa; X indicates the date when moisture starts to build up while Y shows the withdrawal date.</i>	<i>27</i>
<i>Figure 12: Pentad series for equivalent potential temperature (blue series) and saturation equivalent potential temperature (red series) anomalies for MAM season during the year 1991 for Dagoretti station at 850 hPa; X demonstrates the date when moisture starts to build up while Y implies the withdrawal date</i>	<i>28</i>

Figure 13: Time series for actual and predicted rainfall onset (a) and cessation (b) for Narok station using equivalent and saturated equivalent potential temperature anomalies at 700hPa during the MAM season 37

Figure 14: Time series for actual and predicted rainfall onset(a) and cessation (b) during MAM season and actual and predicted rainfall onset(c) and cessation (d) for Wajir during OND season: using equivalent and saturated equivalent potential temperature anomalies 700hPa 38

Figure 15: Time series for actual and predicted rainfall onset(a) and cessation (b) during MAM season and actual and predicted rainfall onset(c) and cessation (d) for Wajir during OND season: using equivalent and saturated equivalent potential temperature anomalies 850 hPa 39

Figure 16: Time series for actual and predicted rainfall onset (a) and cessation (b) for Kisumu using equivalent and saturated equivalent potential temperature anomalies at 700hPa OND season..... 39

Figure 17: Time series for actual and predicted cessation for Moyale using equivalent and saturated equivalent potential temperature anomalies at 850 hPa OND season 40

LIST OF TABLES

Table 1: Rainfall stations for the study area for MAM and OND seasons.....	15
Table 2: Comparison of onset of rains and commencement of moisture build up dates in pentads for Dagoretti Station at 850hPa for the present study and Kerandi (2008) during MAM and OND seasons	29
Table 3: Comparison of onset of rains and commencement of moisture build-up dates in pentads for Dagoretti station at 700hPa for the present study and Kerandi (2008) during MAM and OND season	30
Table 4: Predicted rainfall onset in pentads obtained using Actual Rainfall Onset and equivalent potential temperature anomaly ($\theta_e > 0$) in Pentads during MAM season, at 850-hPa for Dagoretti station	31
Table 5: Predicted rainfall onset in pentads using Actual Rainfall Onset and equivalent potential temperature anomaly ($\theta_e > 0$) in Pentads during MAM season, at 700-hPa for Dagoretti station.....	32
Table 6: Predicted rainfall onset in pentads using Actual Rainfall Onset and equivalent potential temperature anomaly ($\theta_e > 0$) in pentads during MAM season, at 850-hPa for Kisumu station	33
Table 7: Determination of Predicted rainfall onset in pentads using Actual Rainfall Onset and $\theta_e > 0$ in pentads during MAM season, at 700-hPa for Kisumu station	34
Table 8: Determination of Predicted rainfall onset in pentads using Actual Rainfall Onset and $\theta_e > 0$ in pentads during MAM season, at 700-hPa for Marsabit station.....	35
Table 9: Times lags in Pentads for MAM and OND season at 850hPa and 700hPa level for the stations used	36
Table 10: Pearson Correlation Coefficient demonstrating the relationship between Actual and Predicted onset, and Actual and Predicted Cessation for MAM and OND obtained using equivalent potential temperature and saturation equivalent potential temperature at 700hPa and 850hPa levels. The values in bold are the significant values at 5% significant level.	41

ABBREVIATIONS AND ACROYNMS

CC	Correlation Coefficient
CHIRPS	Climate Hazards Infrared Precipitation with Stations
CHPclim	Climate Hazards Group Precipitation climatology
CS	Cessation
CWR	Crop Water Requirement
EA	East Africa
ECMWF	European Centre for Medium-Range Weather Forecasts
EEA	Equatorial East Africa
ENSO	El~Nino Southern Oscillation
ERA	European Re-Analysis
FAO	Food Agriculture Organization
GDP	Gross Domestic Product
IOD	Indian Ocean Dipole
IRP	Infrared Precipitation
ITCZ	InterTropical Convergence Zone
JJA	June-July-August
LRS	Length of Rainy Season
MAM	March-April-May
MJO	Madden Jullian Oscillation
NaN	Not a Number
NHMS	National Hydrological and Meteorological Services
OND	October-November-Decemberh
OR	Onset of Rains

PCA	Principal Component Analysis
PC	Principal Component
QBO	Quasi-Biennial Oscillation
SLP	Sea Level Pressure
SO	Southern Oscillation
SONDJ	September-October-November-December-January
SST	Sea Surface Temperature

CHAPTER ONE

1.0 INTRODUCTION

1.1 Background of the Study

Rainfall is of importance to countries whose economy is dependent on rain fed economic activities. However, rainfall is extremely variant in spatio-temporally in tropical countries because of the complex interaction of the macro-scale and global atmospheric patterns (Endris *et al.*, 2019). Important rainfall characteristics that influence major livelihoods in most tropical Africa are the onset, cessation, wet and dry spells. The timing of the start and end of rainfall determines the duration of the rain season, which has great influence on crop performance. This information is also paramount to other key sectors like irrigation, disaster risk management, health and hydro-electric power generation, for planning and policy making.

Kenya's economy relies on rain-fed agriculture which contributes approximately 26% of the country's Gross Domestic Product (GDP) and an estimated 65% to the total exports (Bosire, 2019). Over most parts of Kenya, annual cycle of rainfall has a bimodal pattern; the long and short rainfall season which occur from March to May (MAM) and October to December (OND). The Inter-Tropical Convergence Zone (ITCZ) controls the seasons as it migrates from south to north of the hemisphere, the inverse is true. However, parts of western and coastal lowlands region exhibit trimodal rainfall regime, with the third peak occurring from July to August (Omondi, 2015). This is controlled by the meridional arm of the ITCZ as moves from east-west or west-east. Generally, long rainy season provides more rainfall as compared to the short rainy season with a lower year to year variability as observed by Camberlin and Okoola (2003). MAM season has lower predictability as compared to OND season due to complex interactions between the global and regional systems that generate large inhomogeneity in the distribution of rainfall in spatial scale (Ogallo, 1982; Semazzi *et al.*, 1996; Okoola, 1998; Indeje, 2000 ; Camberlin and Philippon, 2002).

Previous studies carried out over East Africa (EA) focused on understanding atmospheric processes and predictability of rainfall seasonally using Sea Surface Temperatures and its derived variables (Mutai, 2000; Mutemi, 2003; Owiti, 2005; Owiti *et al.*, 2008; Nyakwada, 2009). Njau (2006) also used tropospheric circulation variables at upper levels to develop local predictors with intention to improve the skill of seasonal predictability of rainfall.

The long rainy season (MAM) is crucial for most areas in the region especially in maize growing areas that require a longer rainy period. Apart from the agricultural sector, the knowledge on rainfall intraseasonal characteristics is also important to other rainfall dependent sectors to ensure reliable and effective economic planning. Most decisions that take place on local scale such as on-farm management require information on the rainfall intra-seasonal characteristics (Barron *et al.*, 2003).

Over time, there has been notable improvement in seasonal forecasting through unrelenting research and this has aided in planning and management of various climate sensitive socio-economic activities in Kenya (Njau, 2006, Kipkogei *et al.*, 2017 and Otieno *et al.*, 2020). However, there has been limited research on developing operational techniques for forecasting rainfall characteristics intra-seasonally, importantly, the start and end of rains. This study therefore focuses on the use of tropospheric moisture accumulation variables to potentially predict the commencement and withdrawal of rainfall over Kenya, in order to reduce the uncertainties.

1.2 Statement of the Problem

Rain-fed agriculture is majorly relied on by the populace in the study domain for their economic prowess. Intraseasonal rainfall characteristics that are significantly related to crop performance are the start and end dates of rainfall. These intraseasonal rainfall characteristics are the lead determinants of the crops to be grown, farming systems, sequence and proper timing of operations. The rainfall commencement and withdrawal dates determine the duration of the rain season which is critical in water resource planning and management since water scarcity is a common issue in Kenya, and is usually attributed to rainfall uncertainties. However, determining the start and end dates of rainfall have posed a challenge because of their high interannual variability. The current approach used by the National and Hydrological Meteorological Services (NHMSs) in Kenya, which is the identification of analogue years (season) has some limitations since the two seasons cannot evolve perfectly in a similar way.

This study aims at developing time lags of onset and cessation of rainfall at station level using equivalent and saturated equivalent potential temperature anomalies for both seasons in order to understand interannual variability of the start and withdrawal dates of rainfall. Equivalent and saturated equivalent potential temperature both serve to monitor the degree of atmospheric

warmness and moistness in any locality (Kerandi, 2008). Previous studies have focused on seasonal prediction of rainfall totals and the linkage to teleconnections (Owiti *et al.*, 2008; Nyakwada, 2009; Bahaga *et al.*, 2015) but minimal studies have been done on intraseasonal rainfall characteristics (Nicholson, 2017). It is crucial to understand intraseasonal rainfall characteristics in order to improve knowledge on the behavior of rainfall locally. This will enhance the accuracy of forecast thus building resilience among rainfall dependent sectors and communities consequently reducing vulnerability to extremes.

1.3 Objective of the Study

This study aims to assess the potential of predicting onset and cessation dates of seasonal rainfall in Kenya using moisture accumulation in the Troposphere during the two rainfall seasons, in order to minimize risks associated with effects of extreme climate variability.

To achieve this overall objective, the following specific objectives were formulated and pursued;

- i. To determine the onset and cessation dates of rainfall and their interannual variability during the two main rainfall seasons over Kenya.
- ii. To identify the commencement and withdrawal dates of moisture accumulation using the tropospheric circulation variables.
- iii. To evaluate the linkage between the rainfall onset and cessation dates and the moisture build up and depletion dates

1.4 Justification of the Study

The amount and distribution of rainfall affects the type of farming activities carried out in an area. Late start and/or early end of seasonal rainfall during the growing season may adversely affect agricultural yields. Crop yields may also be diminished by high prevalence of dry spells in between the growing period. For farmers to plan for farming activities, knowledge on the onset, cessation temporal and spatial variation of seasonal rainfall are vital. The study on the onset and cessation using equivalent potential temperature and saturated equivalent potential temperature which are conservative parameters in both dry and saturated adiabatic conditions is necessary as rainfall is highly heterogeneous. Variation in the dates of onset and cessation disrupt crop development and may result to low yields. Over Katumani station in Eastern Kenya, Stewart and Hash (1982) observed that 20-days delay in onset of long rains result to 25-30% decrease in maize yield. Therefore, dependable prediction of both the onset and cessation prior to the start of

rains is important as it gives effective and reliable information for planning of agricultural and water resources activities.

1.5 Domain of the Study

The area of study is Kenya (Figure 1). It lies at the equatorial region and is enclosed by longitudes 34°E to 42°E and latitudes 5°N to 5°S with an area of 582,646 square kilometers. It borders Uganda to the west, South Sudan to the North West, Ethiopia to the North, Tanzania to the South, Somalia and the Indian Ocean to the East. The study region is dotted with extensive geographical features like escarpments, mountains, deserts, plateaus, lakes, forests among other features. The water bodies that are found within the area of study include Lake Victoria, Lake Naivasha, Lake Nakuru, Lake Bogoria and Lake Baringo among other inland lakes. These features result in the heterogeneity of rainfall in that climatological average rainfall totals vary significantly. Gitau (2011) alluded that, over the highlands and near the large water masses, high average rainfall totals at monthly time scale occur while the Eastern and northern Kenya receive minimal rainfall totals.

The existence of the Rift Valley that stretches from the north to the south across the country and the Turkana channel provides an environment where both local and global systems interact to develop a climate that shows high variability in both space and time.

Most regions in the study domain experience bimodal kind of rainfall; the long rainy season well known as MAM and short rainy season known as OND season. The bimodal regime is affected by the ITCZ system as it moves from north-south. As noted by Asnani (1993), this system is the major large-scale system that controls the MAM and OND seasonal rainfall over the tropics. However, the western and coastal region experience the middle rains in June-August (JJA) portraying a trimodal regime. The trimodal regime is associated with the meridional arm of the ITCZ which results from the convergence of moist westerlies and the easterlies winds from the Atlantic and Indian Ocean respectively. Its fluctuation occurs east-west direction. An easterly extent this system is observed in July to August, and it's linked to the eastward incursion of the westerlies from the Atlantic Ocean which has led to the rainfall received over the region during this season.

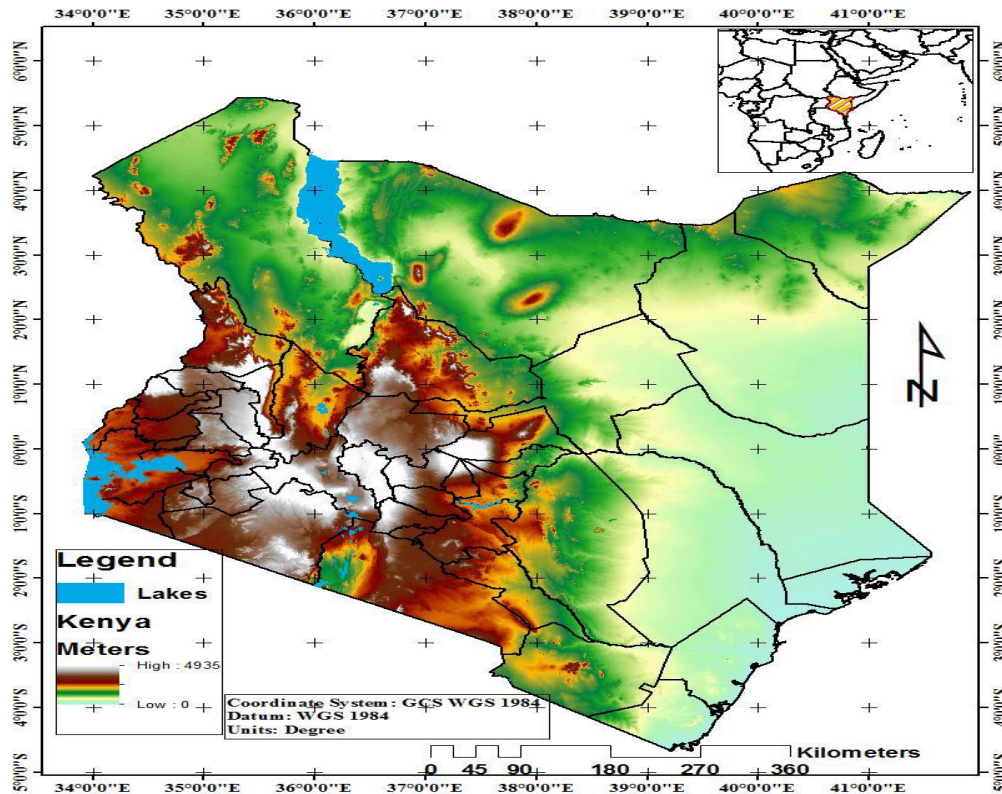


Figure 1: Digital elevation map for Kenya showing physical features. The lakes are in blue and elevations rise from the coast westwards (Omondi, 2015)

The variation of rainfall spatially and temporally over Kenya is influenced by the global, regional and the local scale systems. Mukabana and Piekle (1996) have showed that daily changes of rainfall in the region are as a result of synoptic scale flows, mesoscale flows and their interactions.

Systems that drive the seasonal rainfall over the study region are the Intertropical Convergence Zone (ITCZ), Indian Ocean Dipole (IOD), Madden Jullian Oscillation (MJO), jet streams, El Niño Southern Oscillation (ENSO), mesoscale factors among others. Notable evidence on the effects of Madden Jullian Oscillation on within season rainfall variability has been done by Pohl and Camberlin (2006) over Kenya. They alluded that it influences the variability of the long rains by acting as triggering mechanism for early onsets as well as extreme wet events earlier in the season. Moreover, during the short rains, the system shows strength at $120^{\circ}(10^{\circ})$ linking with dry (wet) spells at the coastal regions of East Africa. Omeny *et al.*, (2008) demonstrated that MJO

can skillfully predict the within season variance of rainfall across the western region of East Africa.

Mutai and Ward (2000) also illustrated that the anomalies of the winds pulse in west direction. It develops approximately five days prior to the respective rainfall event across the Greater Horn of Africa (GHA) region in the Equatorial Atlantic Ocean. The wind pulses in some cases have a strength ranging 2-5 meters per second. It coincides with the rainfall events themselves. Further observation has indicated a tendency for anomalous near-surface easterlies before the rainfall event, which strengthens over the Indian Ocean portraying northeast and southeast trade winds as a stronger onshore component.

Camberlin and Okoola (2003) studied the association between onset time series and coupled ocean-atmospheric large-scale patterns over East Africa. The study concluded that year to year variation in the long rains onset relate to SST and Sea level Pressure (SLP) patterns but have a varying signal over the Atlantic and Indian Ocean on a monthly time-scale. The study further observed that a warming (cooling) over the South Atlantic (Indian Ocean) is linked with low (high) SLP anomalies. The SLP and SST patterns are favorable for the enhancement of surface divergence and equatorial easterlies which maintains the meridional arm of the ITCZ further west resulting in late onset of the long rains. Moreover, an early onset event occurs when there is an induce instability from an incursion of mid tropospheric northerlies.

Dunning *et al.*, (2016), observed a delayed cessation of about 7 days during El Nino while during the La Nina an early onset of about 5 days was observed over East Africa.

Nicholson, 2016 studying the Turkana low level jetstream over the Northern Kenya found that rainfall is modulated by the system especially during the night hours. The study further concluded that the strong jets suppresses rainfall and is a factor to the prevailing aridity in northeast Kenya.

CHAPTER TWO

2.0 LITERATURE REVIEW

This chapter presents previous studies carried out regarding the subject of interest. It focused on the start and end dates of rainfall based on rainfall data and tropospheric circulation variables. Some of the literature review is presented in the Sub-Section 2.1 and 2.2 below.

2.1 Studies on onset and cessation based on rainfall

Liebmann *et al.*, (2012) described the start and end of rainfall in the study of seasonality of African Precipitation during the year 1996 to 2009 as the day when the daily precipitation consistently exceeds its local annual daily average and retreats when precipitation systematically declines below the value. Over Eastern horn of Africa, biannual regime is experienced with the long rains depicting an average start as early as end of February to early May while the short rains portrayed an average start (average end) from late August to end of October (end of October to late December).

Dunning *et al.*, (2016), extended Liebmann *et al.* (2012) method over Africa in the pursuit for start and end of seasonal rainfall. The authors used 5 observational datasets and ERA-Interim reanalysis in its diagnostics of the start and end of rainfall. Over East Africa, the study showed a delayed (early) cessation during El Nino (La Nina) for the short rains by about 7 days and 5 days respectively. The onset recorded a minimal change.

Marengo *et al.*, (2001), defined the start date of rainfall on a regional basis for different stations of the Amazon Basin. The daily rainfall data was averaged from many stations and the computation of 5-days averages was done to obtain the dates. Onset (cessation) was the pentad in which rainfall was more (less) than 4 mm per day provided that 6 out of 8 previous (succeeding) pentads had means of not more than 3.5 mm per day, 6 of the 8 subsequent (preceding) pentads had daily means exceeding 4.5 mm per day. The authors found that the start of rains progressed southeastwards, with arrival in mid-October, it then progressed towards the mouth of the Amazon, arriving as the year ends. On the contrary, the study also showed that the cessation is early in the southeast with progression to the north. The study further concluded that the withdrawal is slower than onset.

Camberlin and Diop (2003) assessed the rainy season characteristics in Senegal by subjecting the daily rainfall data on principal component analysis. The start (end) date of the rainy season

corresponds to the minimum (maximum) turning point of the accumulated first Principal Component (PC1) score curve attained for that year. The Principal Component Analysis (PCA) method turned out to be useful and provided large scale information about the behavior of the rain season.

Sivakumar (1988) studied the prediction of the seasonality of rainy season potential in Southern Sahelian and Sudanian climatic zones of West Africa. The start of rainfall season was after 1st May when rainfall totalled for three consecutive days was 20 mm or more and dry spell exceeding 7 days should not be experienced within the next 30 days. On the other hand, cessation date was regarded to be a date after 1st September followed by no occurrence of rain for a period of 20 days. The author observed significant relationship between the rain onset date and the duration of the growing season.

In the work of Omotosho (1990) on the start of thunderstorms and precipitation across Kano in northern Nigeria, onset of rainfall is taken as the first four falls of 10 mm or more with dry spells not exceeding 7 days between any two such rains. He showed that the start of agriculturally sufficient and reliable rainfall is related to the vertical wind shears between the surface to mid-troposphere (700-400 hPa). The limitation of the study was the sparse upper-air wind data.

Odekunle (2006) used percentage cumulative approach in the determination of the start and end of convective season over Nigeria. The parameters derived were number of convective days and amount. In regard to this approach, the onset of rainfall was the first point of maximum positive curvature on the graph whereas withdrawal is the last point of maximum negative curvature. The maximum curvature points corresponding to the start (withdrawal) of rainfall were 7-8% (90%) of the rainfall totals annually. The study used graphical method in the determination of mean proportion for the estimation of onset and withdrawal dates annually.

Over East Africa, previous studies on the start and end of rainfall corresponding to the commencement and withdrawal of the seasonal rainfall have been defined in many ways using different thresholds and methodology. Some of the studies reviewed for this study are presented below.

Alusa and Mushi (1974) on their study on the start, end and duration of rainy season, found the commencement of rainfall in many East Africa stations to be the first point of maximum positive

curvature on cumulative rainfall plot equating to the first pentad. The first pentad should have a rainfall total exceeding 1/73 of the yearly average.

Mhita and Nassib (1987) in the determination of the start and end of rainfall over Tanzania, described the start of rains as the first week receiving rainfall of 15mm or more, after a given date basing on the local agro-climatic practices (the start of rainfall is early February for regions with bimodal regimes) and provided that the dry spell does not occur two-week during the next four-weeks. The study failed to unearth if the start and end dates exhibit the same year to year variability over East Africa.

Asnani (1993) provided average start and end of rainfall maps based on the subjective analysis of pentad distribution. The study has some setbacks as it fails to unearth the causes of the year to year variability of rainfall start and end dates across East Africa.

Jolliffe and Sarria-dodd (1994) used pentads to determine the start of rains in tropical climates using stations from Zambia and Uganda. They examined the start of the convective season as the wet pentad with at least 25mm of rainfall with at least 3 days greater or equal to 0.85mm of rain.

Camberlin and Okoola (2003) applied the methodology used by Camberlin and Diop (2003) to depict the start and end of Long rains in Kenya and Tanzania. Basing on Barring (1988) study, the 34 time series were square rooted in order to reduce skewness. PCA (S-mode) was applied on the correlation matrix and a score chosen depicting a dominant mode of variability; in this case PC1. Analysis of the time series for all stations over a period longer than the rainy season, including parts of antecedent and posterior dry seasons, was performed. Using rainfall data of 30 years (1958-1987) the start (end) of rains was taken as minimum (maximum) point values. They observed high variability in the onset and less variability in the cessation.

MacLeod (2018) utilized the Liebmann method in the study of seasonal predictability of the start and end of the East Africa rains. The method defines the start and end as the minima and maxima in the time series plot respectively. The method is outstanding since it is locally applied, it is also appropriate for gridded as well as model data. Macleod (2018) found the mean dates of the start and end of rainfall to be consistent with those obtain by Camberlin and Okoola (2003).

Kerandi (2008) applied the methodology used by Omotosho *et al.*, (2000) to define the start and end of rainfall basing on the crop water requirement (CWR) over Kenya. Kerandi (2008) defined

the start date of rainfall to be the first day of any week cumulating 20mm of rainfall or more, followed by 2-3 other weeks having 50% or more of the weekly CWR. The initial three to four weeks are critical for seeds to germinate, crops establishment and survival in the next twenty days. Therefore, initial heavy rains of greater or equal to 10mm are necessary for the wetness and softness of soils.

Mugalavai *et al.*, (2008), analyzed the commencement and withdrawal of rainfall and the duration of the growing season over Western Kenya for both rainfall seasons (MAM and OND). The study considered daily rainfall data for 26 stations for the period of 15-34 years; Rain software was used to determine both the onset and cessation dates. The appropriate threshold for the onset was 40 mm for a maximum of 4 days while the cessation was determined using the water stress which was assessed by the water stress coefficient, K_s . Cessation of the rainy season was assumed when K_s dropped below 0.40 within the cessation window. The study observed high variability for the start of rainfall dates and low variability for the cessation dates.

Recha *et al.*, (2012) determined the variability, start and end of seasonal rainfall over Tharaka District, Kenya. By adopting Odenkule (2006) approach, he performed percentage mean cumulative on the amount and days of rainfall for three stations: Marimanti (1969-1997), Tunyai (1974-2006) and Chiakariga (1974-1998). Basing on this approach, start date for MAM and OND seasons occurred on the 5th pentads of the month of March and October respectively. The cessation portrayed variability for both the seasons, the cessation occurred on 3rd and 2nd pentad for May and January respectively. The study observed that the onset and cessation depicted high and low variability during MAM and OND respectively.

Micheau *et al.*, (2013) develop a new approach of obtaining onset and cessation based on a multi variate analysis over Kenya and Northern Tanzania. The method combines several rainfall thresholds in a PCA, this is for the purpose of extracting robust signal across space and parameters. The study suggest that the use of stringent thresholds is important in detecting start and end dates for certain conditions. It also increases the signal of year to year variability and spatial consistency regionally. Results obtained suggested that PC1 based on multicomination was more superior in extracting regional scale component of the onset as compared to use of a single, arbitrary combinations of thresholds

Ngetich *et al.* (2014) determined the duration of the growing season, distribution of the precipitation temporally and the start and end dates of rainy season over the Kenyan highlands, majorly on Maara and Meru South Sub-Counties in Tharaka Nithi County and Mbeere North and South Sub Counties in Embu County of the central highlands of Kenya. RAIN software was used in the determination of onset and cessation with the onset date defined as the day with exceedance of 25 mm (30 mm) of the cumulated rainfall recorded in the low altitude (high altitude) area for utmost 3 to 5 successive days. The season lag time was set as 7 days after the start; the threshold for the convective day was taken as 0.85 mm. For the withdrawal date, the criterion used was soil water balance with set threshold of water stress coefficient not exceeding 40%. For the higher altitude region, the onset ranged from 22nd March to end of April while the low altitude portrayed an onset from 16th to 30th March for the long rains. Early start of rainfall was recorded in high altitudes areas whereas the late start was observed in low altitudes areas for the short rains. An unlike the long rains season, less spatial and temporal variability was observed for the short rains.

The studies reviewed has focused on some regions and not all representative stations of the homogenous zones. Moreover, methodology adopted for this study is by Camberlin and Okoola (2003) which has shown superiority compared to other methods (use of rainfall thresholds and agro-climatic definitions) because it extracts co-variability in rainfall for the stations exhibiting variability in time other than merely smoothing the day to day rainfall fields.

2.2 Studies on the onset and cessation of rainfall using tropospheric circulation variables

Many studies have been done with intention to unearth the mechanisms driving the rainfall variability and change on different spatio-temporal scales over East Africa. Studies such as SST and SST-derived variables have been done by Mutai (2000), Mutemi (2003), Owiti (2005), Owiti *et al.*, (2008) and Nyakwada (2009). Okoola *et al.* (2003) examined the relationship between onsets and coupled ocean-atmospheric large-scale patterns. The study concluded that the interannual variance of the onset of long rainy season is associated with SSTs and SLP on monthly timescale. Moreover, Dunning *et al.*, (2016) found the patterns of the start and end of rainfall to be consistent with the progression of the ITCZ and the West African Monsoon. The reviewed work basing on the tropospheric circulation variables was done by Omotosho *et al.*, (2000), Njau (2006) and Kerandi (2008).

Omotosho *et al.* (2000) used surface data to develop long range empirical schemes for Kano, West African Sahel region. The schemes developed were for predicting the dates of the commencement and withdrawal of rainfall, monthly and annual amounts of rainfall. The study was based on fluctuations of equivalent potential temperature which occur due to variations in daily, monthly and seasonal moisture in the summer monsoon flow. The study indicated that the agricultural practices may commence approximately two and half months after the day the anomalies of equivalent potential temperature first become positive for at least 15 days. This signifies the enough moisture build-up related with a well-intensified monsoonal flow. The schemes also forecast end date and the annual amount prior to the start of rains which is useful information purposely for planning in rainfall related activities.

Njau (2006) used the upper tropospheric circulation variables to determine the best set of local predictors for the prediction of rainfall seasons in EA. The observed temperature and geopotential associate well with seasonal rainfall anomalies. The results depicted that an increase in temperature in the upper part of the troposphere increases geopotential height that could be associated with increased moisture convergence and precipitation. On the other hand, cooling at the same level leads to decrease in geopotential height associated with reduced moisture convergence and precipitation.

Kerandi (2008) developed empirical schemes using surface and 700 hPa data for both long and short rain seasons over Kenya using Dagoretti station as the case study. He used equivalent potential temperature and saturated equivalent potential temperature as both serve to monitor the degree of atmospheric warmness and moistness over an area. The study showed that for MAM (OND), the onset of rainfall can be predicted well in advance by 54 and 60 (51 and 58) days for surface and 700 hPa respectively. The prediction is done when the anomaly of equivalent potential temperature becomes positive for 2-3 pentads. He further showed that the cessation can also be forecasted 104 and 106 days for the MAM period and 73 and 71 days for OND, for surface and 700 hPa, prior to the end of rains. This is predicted when maximum separation between equivalent potential temperature and saturated equivalent potential temperature anomaly occurs, linking this scenario to the withdrawal of rainfall.

It is evident from the literature that limited studies has been done using the tropospheric moisture variables to predict the onset and cessation dates of rainfall. The study by Kerandi (2008) was

limited to 2 stations (Dagoretti and Mombasa station) which is a small spatial scale distribution. Therefore, there is need for more research using more dense station network in order to obtain onset and cessation of rainfall dates at local level which this study is addressing.

CHAPTER THREE

3.0 DATA AND METHODOLOGY

This chapter describes the data and the methods used in order to attain the set objectives of the study.

3.1 Data Type and Source

The daily datasets utilized in this study were Climate Hazards InfraRed Precipitation with Stations (CHIRPS) and Temperature and Relative Humidity from European Centre for Medium-range Weather Forecasts (ECMWF) Re-Analysis, ERA-5. The data had already been subjected to quality control and fit for analysis. The CHIRPS data ranged for a period of 38 years (1981-2018) and the Temperature and Relative Humidity were extracted at the surface (850-hPa) and mid-level (700-hPa) for a period of 30 years (1989 to 2018). The 850-hPa level is a zone of low-level moisture and temperature advection; 700-hPa level is a zone of medium level cloud formation, additionally it is a level where most systems are steered by the winds and a region where troughs and ridges are well defined.

3.1.1 Climate Hazards Infrared Precipitation with Stations

The Climate Hazards Infrared Precipitation with Stations is a quasi-global rainfall dataset extending from 1981 to present. It has a resolution of 0.05°, consists of satellite estimates blended with gauged rainfall data to produce gridded rainfall time series.

Dinku *et al.*(2018) assessed the performance of CHIRPS over East Africa, comparatively with other satellite data and showed a better performance with a higher skill, low or no bias and lower random errors. CHIRPS data was extracted for the stations in Table 1. The stations used are the representatives of the homogenous zones for MAM and OND season, for the purpose of achieving the set objective of the study.

Table 1: Rainfall stations for the study area for MAM and OND seasons.

MAM				
Zone	Stations	Latitude	Longitude(⁰ E)	Altitude(m)
1	Lodwar	3.7 ⁰ N	35.57	506
2	Moyale	3.32 ⁰ N	39.02	1097
3	Wajir	1.45 ⁰ N	40.04	244
4	Garissa	0.29 ⁰ S	39.38	147
5	Lamu	2.16 ⁰ S	40.54	30
6	Mombasa	4.02 ⁰ S	39.37	55
7	Voi	3.24 ⁰ S	38.34	597
8	Dagorreti	1.18 ⁰ S	36.45	1798
9	Nanyuki	0.03 ⁰ N	37.02	1905
10	Narok	1.08 ⁰ S	35.5	1890
11	Marsabit	2.18 ⁰ N	37.54	1345
12	Kisumu	0.06 ⁰ S	34.45	1146
OND				
Zone	Stations	Latitude	Longitude(⁰ E)	Altitude(m)
1	Lodwar	3.7 ⁰ N	35.57	506
2	Moyale	3.32 ⁰ N	39.02	1097
3	Mandera	3.56 ⁰ N	35.37	230
4	Wajir	1.45 ⁰ N	40.04	244
5	Kakamega	0.17 ⁰ N	34.47	2133
6	Nakuru	0.16 ⁰ S	36.36	1901
7	Dagorreti	1.18 ⁰ S	36.45	1798
8	Garissa	0.29 ⁰ S	39.38	147
9	Voi	3.24 ⁰ S	38.34	597
10	Mombasa	4.02 ⁰ S	39.37	55
11	Lamu	2.16 ⁰ S	40.54	30
12	Kisumu	0.06 ⁰ S	34.45	1146

3.1.2 Temperature and Relative Humidity

This study sourced temperature and relative humidity datasets from ERA5 re-analysis dataset. The ERA5 data is a 5th generation data assimilated system that is produced by ECMWF and a key element of EU-funded Copernicus Climate Change Services (C3S). It has a high spatial resolution of 0.25° latitude by 0.25° longitude. The observations available are added with forecast to infer the evolution state beneath the surface and the atmosphere. Results by Zhang *et al.* (2016), Albergel *et al.* (2018) and Urraca *et al.* (2018) concluded that ERA5 is superior in representing atmospheric variables as compared to ERA-Interim.

3.2 Methodology

The set specific objectives of the study were achieved using analytical techniques presented and discussed in the subsequent sub-sections: -

3.2.1 Determination of Onset and Cessation Dates of Rainfall

To meet the first specific objective, Camberlin and Diop (2003); Camberlin and Okoola (2003) technique was applied. This technique is built on rainfall anomalies that are cumulated to demonstrate the evolution of the rainy season. The daily CHIRPS data was extracted as 1 grid, 4 grids and 16 grids (For the data extracted from 1 grid, the data was extracted from 4 grid points then spatial averaged; for the 4 grid the data was extracted within a buffer of resolution 0.1*0.1 while for the 16 grids the buffer resolution was 0.15*0.15 basing on the latitude/longitude of the stations in Table 1) in order to reduce biasness. It was then subjected to Principal Component Analysis (PCA-S mode) for the period 1981-2018.

The leading PC1 score time series is subsetted yearly. The first principal component corresponds the major mode of variance in the domain of study. Computation of the cumulative series was performed yearly from 1st February to 30th June and 1st September to 31st January for the MAM and OND seasons respectively for the period of study. PCA has demonstrated uniqueness relative to simple averaging as it extracts co-variability in rainfall for the stations exhibiting variability in time other than merely smoothing the day to day rainfall fields. In this case the start (end) dates of rainfall were taken as minimum (maximum) point values.

3.2.2 Identification of moisture commencement and withdrawal pentads

To achieve this objective pentad time series plots were used to identify the commencement and withdrawal dates of moisture. This was achieved by identifying the date, X , when equivalent potential temperature anomaly become positive for at least 2-3 pentads, which indicates the start of supply of enough moisture. The end of moisture supply, withdrawal date, was identified as the point Y which represents maximum separation between equivalent potential temperature and saturation equivalent potential temperature anomalies, which imply the date of the highest moisture build-up before the start of the rain season. Empirical formulas were used to compute saturated vapor pressures (e_s), vapor pressure (e), specific humidity (q), saturated specific humidity (q_s) and potential temperature in order to determine the equivalent and saturated equivalent potential temperature as suggested by Omotosho *et al.*, (2000).

The Clausius-Clapeyron equation was used to compute saturation vapor pressure (e_s) and vapor pressure (e) in Equation 1 and 2.

$$e_s = e_{s0} * \exp \left[\frac{L_v}{R} * \left[\frac{1}{T_0} - \frac{1}{T} \right] \right] \dots\dots\dots (1)$$

$$e = e_{s0} * \exp \left[\frac{L_v}{R} * \left[\frac{1}{T_0} - \frac{1}{T_d} \right] \right] \dots\dots\dots (2)$$

where $e_{s0}=6.11\text{mb}$, $T_0=273.16\text{ K}$, $R=461.5\text{J/Kg/K}$ is the specific gas constant for water vapor, $L_v = 2.5 * 10^6\text{ J/Kg}$ is the latent heat of vaporization, T and T_d is temperature and dew point temperature respectively.

To compute q_s and q , Equations 3 and 4 were used;

$$q_s = \epsilon_1 e_s / (P - \epsilon_2 e_s) \dots\dots\dots (3)$$

$$q = \epsilon_1 e / (P - \epsilon_2 e) \dots\dots\dots (4)$$

where $\epsilon_1=0.622$, e_s is the saturation vapour pressure and e is the vapour pressure from Equation (1) and (2) above, $\epsilon_2=0.378$ and P is pressure.

To evaluate the potential temperature, Poisson's equation shown in Equation 5 was utilized;

$$\frac{T_0}{T} = \left(\frac{P_0}{P} \right)^{\frac{R}{C_p}} \dots\dots\dots (5)$$

where $\frac{R_d}{C_p} = 0.286$ and R_d is the gas constant and C_p is the specific heat for dry air at constant pressure and P_0 is 1000mb.

To calculate saturation equivalent potential temperature, Equation 6 was used;

$$\theta_{es} = \theta \exp (L_c q_s / C_p T) \dots\dots\dots (6)$$

In Equation (6), L_c is the latent heat of condensation.

Equivalent potential temperature is computed using Equation 7 as follows;

$$\theta_e = \theta \exp (L_c q / C_p T_v) \dots\dots\dots (7)$$

where q is the specific humidity and T_v is the virtual temperature.

$$T_v = T (1 + 0.61q) \dots\dots\dots (8)$$

The fluctuations of these parameters were computed in order to assess the moisture supply in the atmosphere. To obtain the fluctuation for equivalent potential temperature and saturation equivalent potential temperature Equations 9 and 10 were used

$$\hat{\theta}_e = \theta_e - \bar{\theta}_e \dots\dots\dots (9)$$

$$\hat{\theta}_{es} = \theta_{es} - \bar{\theta}_{es} \dots\dots\dots (10)$$

In this study, the criterion for variable $\hat{\theta}_e$ and $\hat{\theta}_{es}$ were utilized as follows:

- i. The date, X, when $\hat{\theta}_e > 0$ (become positive) for at least 2-3 pentads, indicates the start of supply of abundant moisture. This is used to predict the onset of rainfall.
- ii. The point Y represents maximum separation between $\hat{\theta}_e$ and $\hat{\theta}_{es}$ time series, which imply the date of the highest moisture build-up before the start of the rainy season. These criteria were used to predict the end of rainfall.

These criteria (i and ii) were used to identify the moisture build up and depletion dates.

3.2.3 Evaluation of the linkage between rainfall onset and cessation dates, and the moisture build-up and withdrawal of moisture dates

This specific objective was achieved by developing the time lags for the prediction of the start and end of rainfall. It was achieved by first determining the start and end dates of rainfall in the first objective then converted to pentads; actual rainfall onset and cessation in pentads, for the purpose of consistency with the pentad data. Then followed by the identification of moisture accumulation (X) and withdrawal (Y) dates in a time series plots in objective two. The difference between the date (X), when equivalent potential temperature anomalies first become positive ($\hat{\theta}_e > 0$) for at least 2 or 3 pentads, and the actual rainfall onset in pentads, for each year, were averaged. This scenario, $\hat{\theta}_e > 0$, is considered because it indicates the start of moisture supply thus important moistener in the atmosphere (Omosho *et al.* 2000). The difference between Y (maximum difference obtained between equivalent potential temperature and saturation equivalent potential temperature anomalies) dates and the actual rainfall cessation dates, for each year were averaged. The averaged values obtained are the time lags.

The time lags obtained are then added to the start and end pentads of the moisture build up to obtain the predicted onset and cessation of rainfall. Graphical method which involved the plotting of the pentads against the years was used to demonstrate the interannual variability; correlation analysis was used to quantify the relationship between the two variables.

The Pearson's correlation coefficient (r_{xy}) used has the limits +1 and -1 which implies that when r_{xy} is close to +1(-1) there is a strong positive (negative) linear relationship. Zero values show no relationship.

$$r_{xy} = \frac{\sum_{i=1}^n (X_i - \bar{X})(Y_i - \bar{Y})}{\sqrt{\sum_{i=1}^n (X_i - \bar{X})^2 (Y_i - \bar{Y})^2}} \dots\dots\dots (11)$$

In equation 11, r_{xy} is the correlation coefficient between X and Y, in this case the variables represent the actual and predicted onset, and the actual and predicted cessation respectively.

This method was used to assess the relationship between the actual and predicted onset, and the actual and predicted cessation for the MAM and OND seasons.

Upon computing the correlations, their significance was assessed using the student t- test. This involves computing the t- test value and comparing it with the critical t value from the t-tables at 95% confidence level (5% significance level). Satisfactory results are interpreted as a 95% assurance that the variables considered are not correlated by chance. The mathematical formula for computing the t values is given as follows;

$$t_{N-2} = r \sqrt{\frac{N-2}{1-r^2}} \dots\dots\dots (12)$$

Where N is the data length and N-2 is the degrees of freedom, r is the correlation coefficient and t_{N-2} is the student t- test distribution.

CHAPTER FOUR

4.0 RESULTS AND DISCUSSIONS

This chapter presents and discusses results obtained in the study basing on the methodologies used to accomplish the set specific objectives in Section 1.3.

4.1 Onset and Cessation dates of Rainfall

The start and end dates of rainfall were achieved by subjecting the data of the selected stations in the homogenous zones to the methodology set in Section 3.2.1. Figure 2 shows some plots that demonstrate how the determination of the start and end dates of rainfall. Time series for both seasons displays a decreasing curve which corresponds to the decreasing atmospheric moisture during the preceding dry season, then an increasing curve corresponding to an increasing moisture during the preceding a dry season and at the end a decreasing curve. The onset date corresponds to the minimum turning point of the accumulated PC1 score curve attained for that year. Alternatively, the maximum turning point of the accumulated PC1 score curve denotes a cessation.

Figure 2a depicts an onset (cessation) on 3rd March (28th April) for Marsabit station for the MAM season while Figure 2b depicted an onset (cessation) on 27th October (4th January) for the OND season during the year 1986 for Dagoretti station.

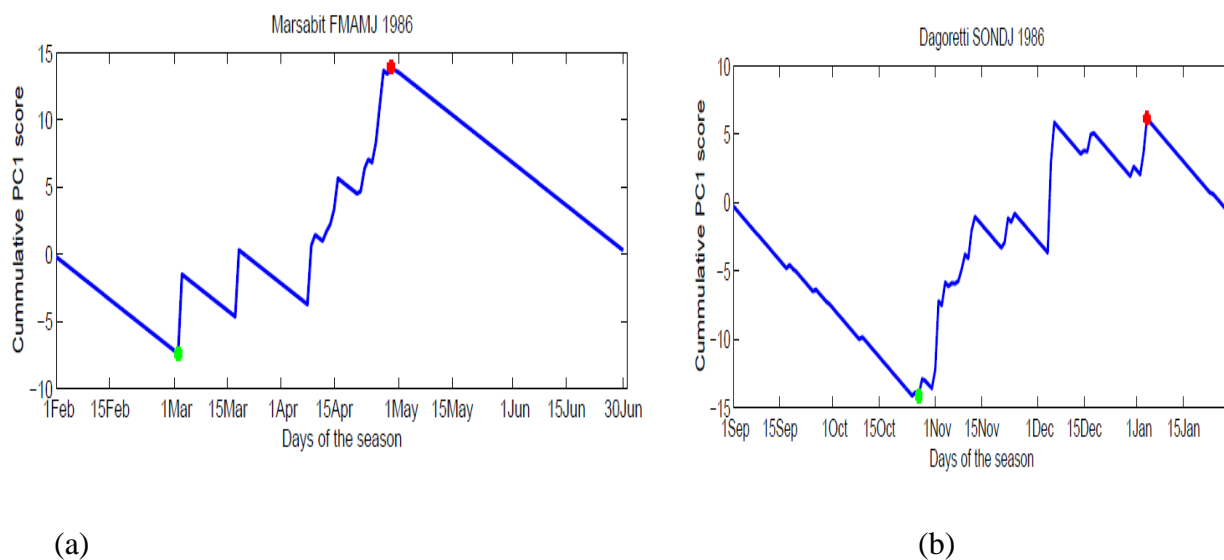


Figure 2: Onset (green dot) and cessation (red dot) date of rainfall at (a) Marsabit during MAM season and (b) Dagoretti during OND season for the year 1986

4.1.1 Interannual Variability of the Dates of Onset and Cessation of Rainfall

Figures 3-5 and Figures 6-8 show the year to year variability of the commencement and withdrawal dates of rainfall for the MAM and OND season respectively, for the stations used in the study. During the MAM season it was observed that the start of the rainfall season extended from mid-February to mid-April over Kisumu, with an earliest onset in the year 2010. The rainfall cessation dates ranged from mid-April to end of June (15thApril-30thJune).

Over Marsabit an early onset occurred from mid to late February during the year 1990, 2010 and 2018. Cessation was observed to start from mid-April to the beginning of May. On the other hand, Voi recorded an early onset beginning February during the year 1989 and 2014. Early cessation experienced in this region ranged from late March to 22nd of May. The stations over the Eastern region (Marsabit, Moyale, Garissa, Voi and Wajir) have a commonality in that they all recorded a shorter rainy season.

Okoola (1998) using Kakamega and Marsabit stations as a representation for western and northern Kenya, obtained an onset of rainfall for the MAM season to be pentad 15 (12-16 March) for the year 1981. These results were consistent with the work done by Camberlin and Okoola (2003) except for the cessation which demonstrated discrepancies. The present study obtained an onset to be 10th March for Marsabit, though discrepancy of 2 days was observed which may be attributed to the time scale used. The current study used daily time scale while Okoola (1998) used pentads. This study determined rainfall onset station by station whereas Camberlin and Okoola (2003) obtained one onset date for the whole of Kenya and Northern Tanzania.

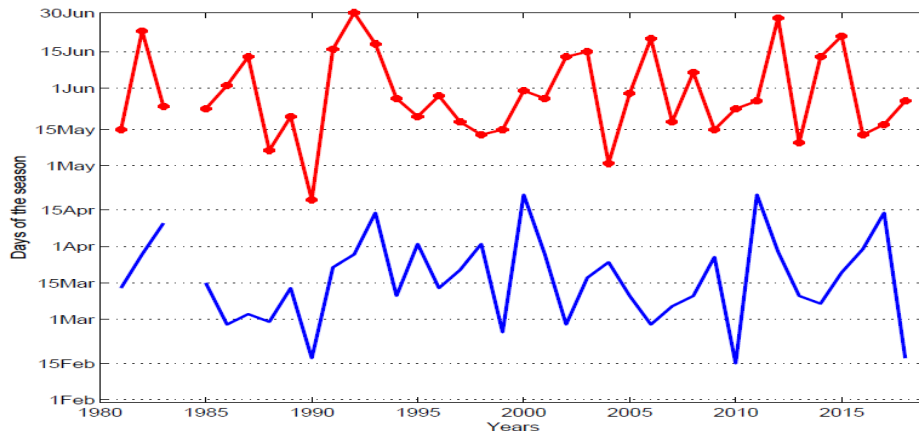


Figure 3 : *Interannual variability of rainfall onset (blue time series) and cessation (red time series) over Kisumu during MAM season from 1980 to 2018*

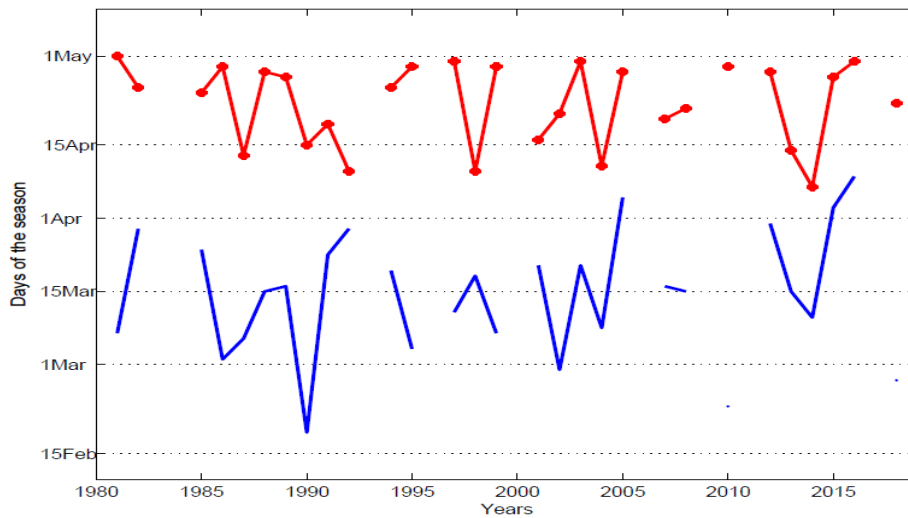


Figure 4: *Interannual variability of rainfall onset (blue time series) and cessation (red time series) over Marsabit during the MAM season from 1980-2018*

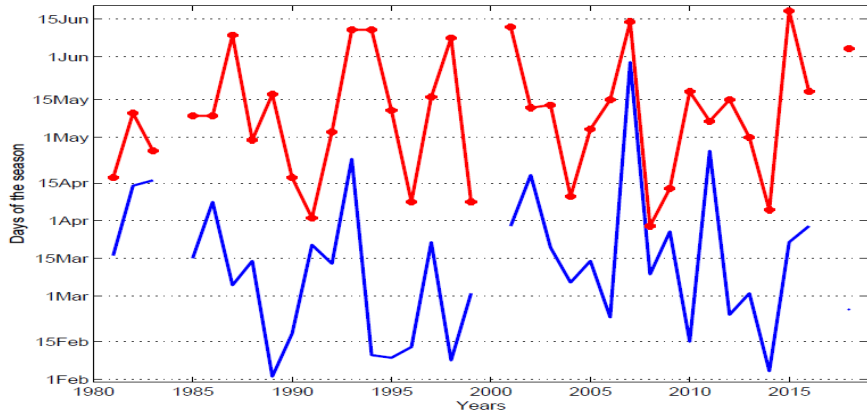


Figure 5: Interannual variability of rainfall onset (blue time series) and cessation (red time series) over Voi during MAM season from 1980-2018

During the OND season the onset (cessation) of rainfall ranged from September-November (September-January). Kakamega station which spatially exists in the western region of the study domain portrayed an onset which ranged from early October to end of November with late onset experienced in the year 1999 and 2003. Some years recorded neither onset nor cessation as demonstrated by Figures 3-8. This is because the threshold for the duration of rainfall was not met; the duration of rainfall was taken as cessation minus onset and should be greater than 10 days. Few missing start and end dates of rainfall were observed for Kisumu, Kakamega, Lamu and Mombasa. These stations are near the water masses; stations at a long distance from water bodies had several years without distinct dates of onset and withdrawal of rainfall. The observations made infer that the proximity to the water bodies have had an influence on the criteria.

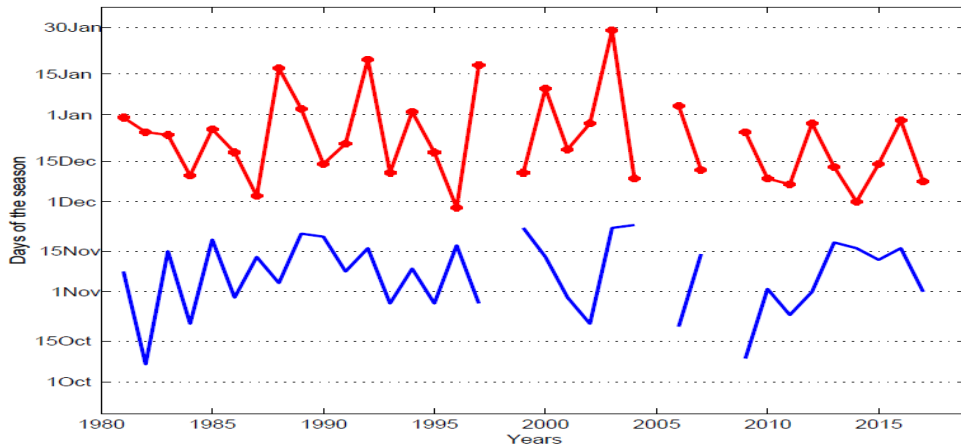


Figure 6: Interannual variability of rainfall onset (blue time series) and cessation (red time series) over Kakamega during the OND season from 1980-2017

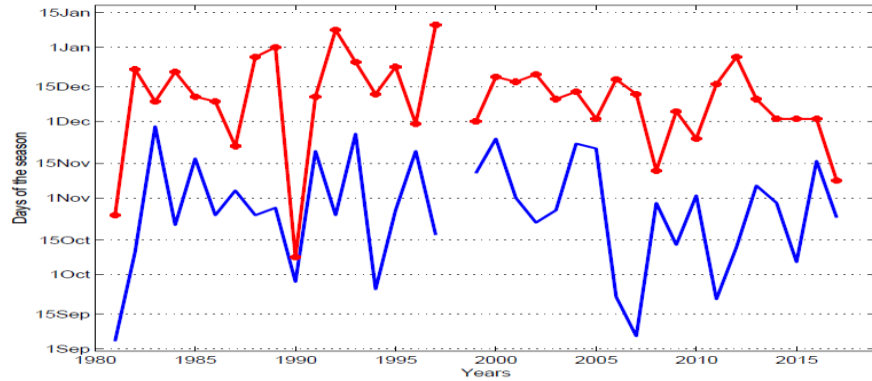


Figure 7: Interannual variability of rainfall onset (blue time series) and cessation (red time series) over Lamu during the OND season from 1980-2017

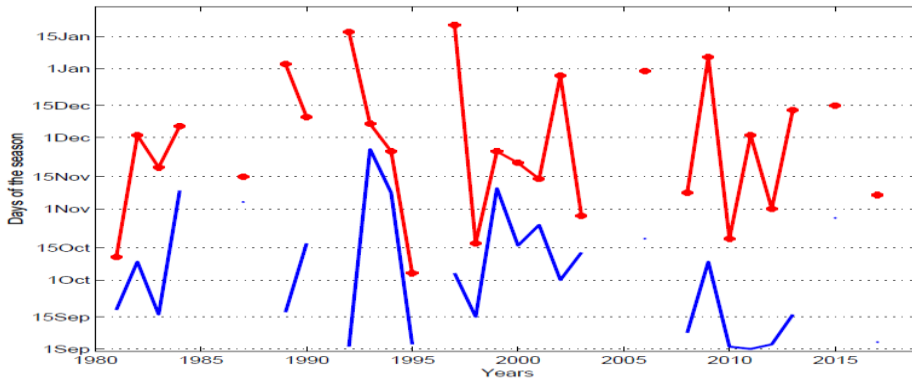


Figure 8: Interannual variability of rainfall onset (blue time series) and cessation (red time series) over Nakuru during the OND season from 1980-2017

***NB: The gaps in the time series (Figures 3-8) represents the missing onset**

4.1.2 Spatial distribution of the mean start and end dates

Figures 9 and 10 show the spatial distribution of mean start and end dates of rainfall for the year 1981-2018 for the MAM season and 1981-2017 for the OND season. Mean onset ranged from 15th March to 8th April while mean cessation occurred from 20th April to 29th May for the long rains (MAM). The mean onset of rainfall during the short rain season (OND) ranged from 23rd September to 11th November whereas mean cessation ranged from 28th November to 27th December.

The stations in the western region (Kisumu, Kakamega and Narok) depicted a longer rainy season. This may be attributed to their geographical location favored by Lake Victoria and Congo air mass which act as a continuous moisture supply. The rainfall onset in the northern

region progresses northwards during MAM and southward progression during the OND season. The pattern observed shows consistency with the physical driver of African seasonal precipitation namely the ITCZ. Over the northern region, the rains are observed to start late and end early. Generally, early onset observed in western region is influenced by the moist westerlies influx from the Atlantic Ocean and the moist Congo air masses while at the coastal region most large-scale systems like south easterly monsoons are active. The systems drive warm moist airmasses towards the land during the OND season favoring an early onset of rainfall.

Kerandi (2008) using Crop Water Requirement (CWR) methodology, obtained mean onset for Nairobi (using Dagoretti station) and Mombasa (using Moi International Airport) to be 25th March and 4th April respectively whereas the cessation occurred late; 8th and 20th June. The present study shows some inconsistency in onset with a variability of 5 and 1 day(s), which might not have much impact while the cessation demonstrated a variability of approximately 1 month. The reason for the variability in the cessation cannot be explained.

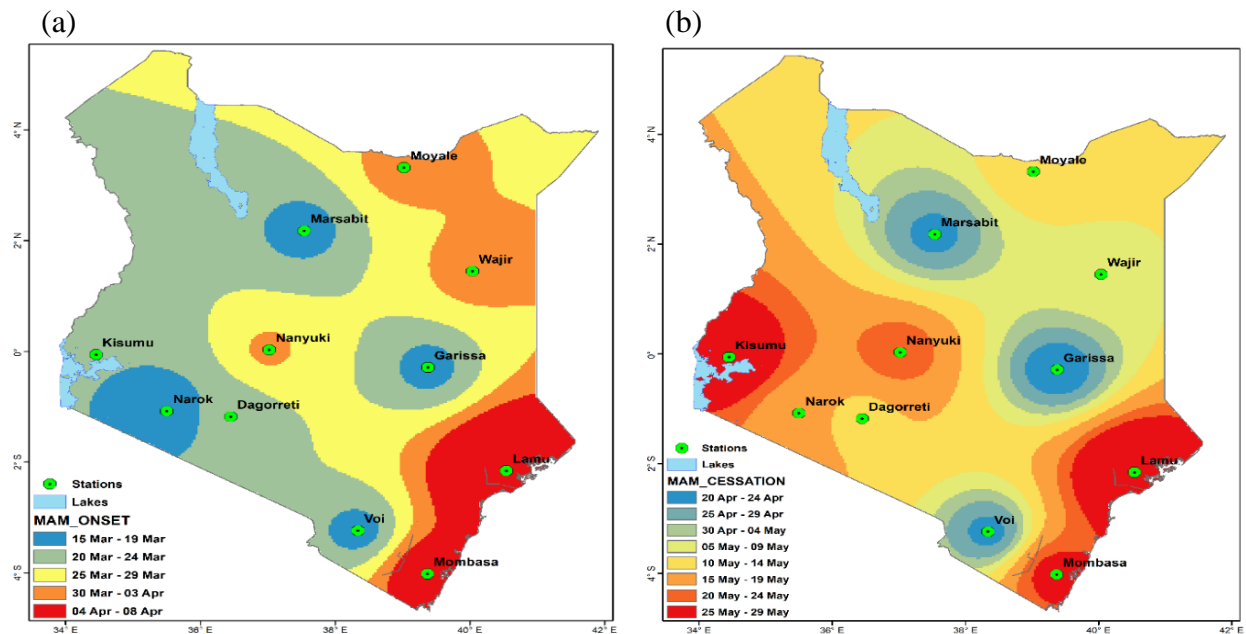


Figure 9: Spatial distribution of mean onset (a) and cessation (b) dates of rainfall during the MAM season for the period 1981-2018 over Kenya

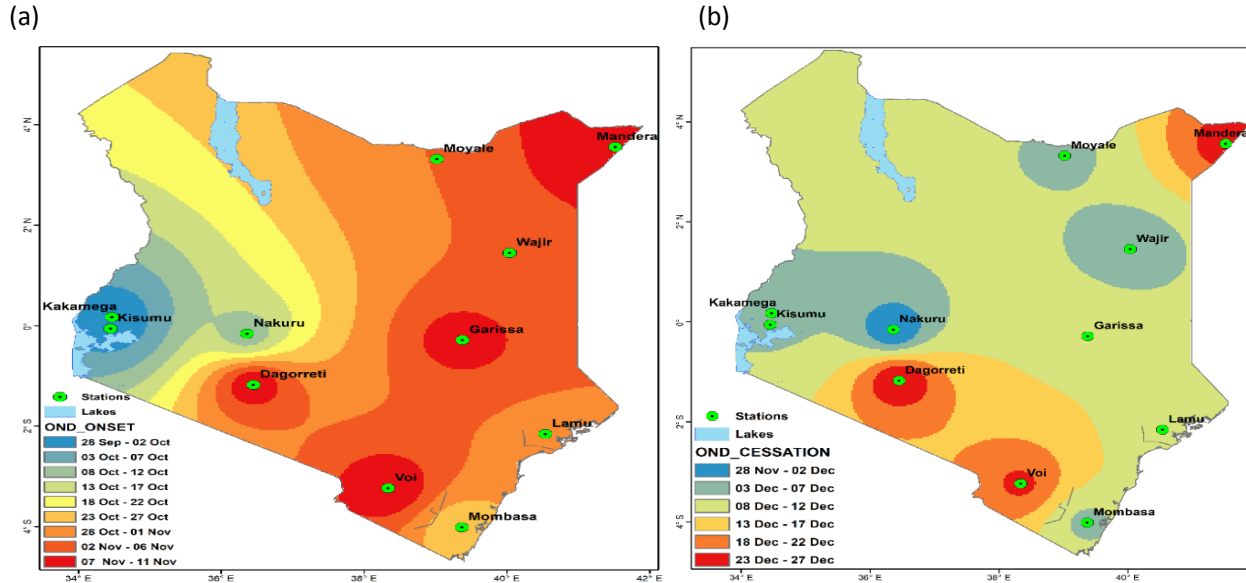


Figure 10: Spatial distribution of mean onset (a) and cessation (b) dates of rainfall during the OND season for the period 1981-2017 over Kenya

4.2 Dates of Commencement and Withdrawal of Moisture

The commencement and withdrawal of moisture dates was achieved using the criteria set in Section 3.2.2. Figures 11 and 12 illustrate how the commencement and withdrawal dates of moisture in the atmosphere were identified using Dagoretti station. For the year 1989, the values for X(Y) were identified as pentads 7(12) whereas pentads 17(18) were obtained for the year 1991.

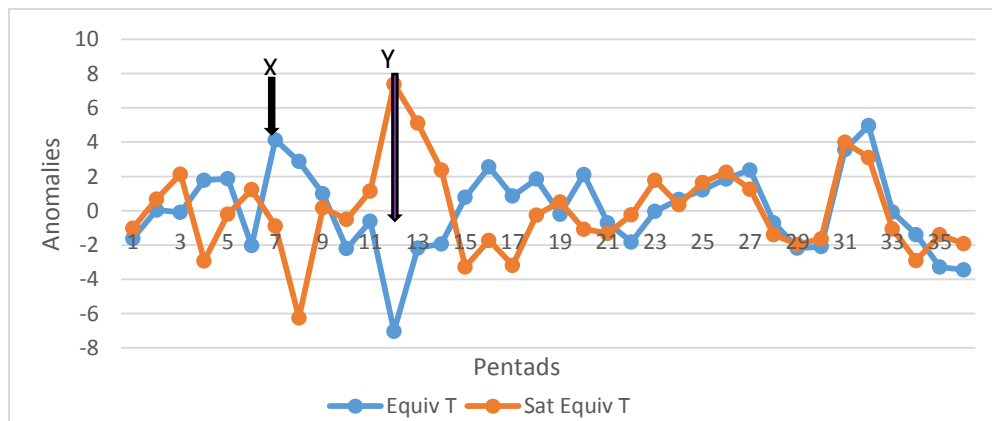


Figure 11: Pentad series for equivalent potential temperature (blue series) and saturation equivalent potential temperature (red series) anomalies for MAM season during the year 1989 for Dagoretti station at 850 hPa; X indicates the date when moisture starts to build up while Y shows the withdrawal date.

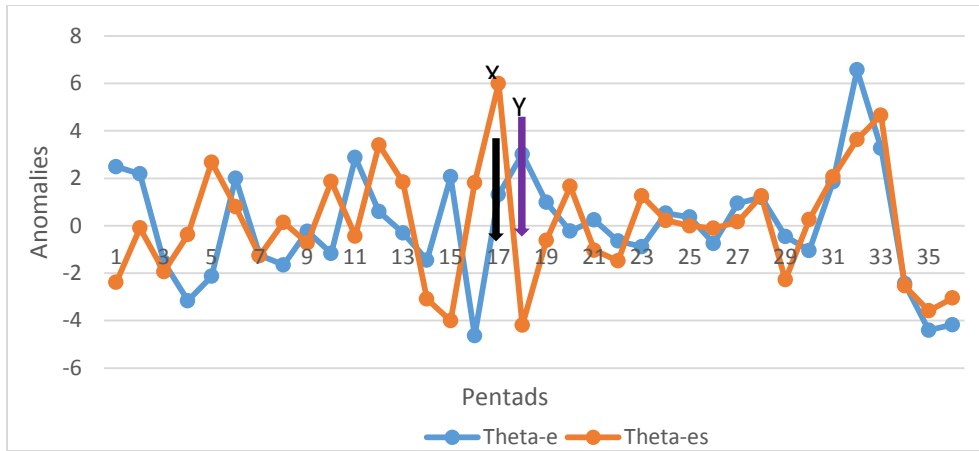


Figure 12: Pentad series for equivalent potential temperature (blue series) and saturation equivalent potential temperature (red series) anomalies for MAM season during the year 1991 for Dagoretti station at 850 hPa; X demonstrates the date when moisture starts to build up while Y implies the withdrawal date

Tables 2 and 3 compare the results on onset of rains and moisture accumulation dates in pentads obtained in this study with that of Kerandi (2008) for 850-hPa and 700-hPa for Dagoretti station. The onsets of rains in pentads were generated from the onset dates in objective one, where the 5-day means were computed for the purpose of consistency with the moisture accumulation dates in objective two. Disparities were observed for both seasons and levels except for the commencement of moisture accumulation dates during the year 1989, 1992, 1998 and 2003 at 850-hPa and the year 2002 at 700-hPa during the MAM season. The difference observed may be attributed to the source of data and the conversion from dates to pentads. This study utilized satellite data while Kerandi (2008) used observed data from radiosonde.

Table 2: Comparison of onset of rains and commencement of moisture build up dates in pentads for Dagoretti Station at 850hPa for the present study and Kerandi (2008) during MAM and OND seasons

MAM (850hPa)				
	Current study		Kerandi (2008)	
	Onset of rains in pentads	$\theta_e > 0$ (in Pentads)	Onset of rains in pentads	$\theta_e > 0$ (in Pentads)
1989	10	7	15	7
1990	4	NaN	13	2
1991	NaN	17	17	7
1992	12	3	19	3
1998	14	9	19	9
2002	6	NaN	13	8
2003	16	8	21	8
2004	8	1	18	6
OND				
	Onset of rains in pentads	$\theta_e > 0$ (in Pentads)	Onset of rains in pentads	$\theta_e > 0$ (in Pentads)
1989	14	2	26	15
1990	13	10	24	16
1991	17	22	26	7
1992	13	17	24	21
2001	NaN	3	23	14
2002	14	8	22	5
2003	11	14	22	13
2004	14	4	22	12

Table 3: Comparison of onset of rains and commencement of moisture build-up dates in pentads for Dagoretti station at 700hPa for the present study and Kerandi (2008) during MAM and OND season

MAM (700hPa)				
	Current study		Kerandi (2008)	
	Onset of rains in pentads	$\theta_e > 0$ (in Pentads)	Onset of rains in pentads	$\theta_e > 0$ (in Pentads)
1989	10	4	15	1
1990	4	NaN	13	3
1991	NaN	6	17	5
1992	12	3	19	7
1998	14	8	19	NaN
2002	6	3	13	3
2003	16	NaN	21	8
2004	8	1	18	6
OND				
	Onset of rains in pentads	$\theta_e > 0$ (in Pentads)	Onset of rains in pentads	$\theta_e > 0$ (in Pentads)
1989	11	2	26	10
1990	13	NaN	24	11
1991	17	6	26	5
1992	13	3	24	9
2001	NaN	5	23	7
2002	14	3	22	5
2003	11	NaN	22	7
2004	14	1	22	14

***NaN in Tables 2-3 implies missing, resulting from the criteria not met**

4.3 Linkage between Rainfall Onset and Cessation dates; and the Start and End dates of Moisture accumulation

The link between the start and end dates of the seasonal rainfall, and the commencement and withdrawal dates of moisture were achieved following the criteria set in methodology 3.2.3. Tables 4-8 demonstrate the actual and predicted rainfall onset in pentads for Dagoretti, Kisumu and Marsabit station during the MAM season. The mean values obtained in Table 9 are the time lags which were added to X and Y values to obtain the predicted rainfall onset and cessation. The time lags for Dagoretti are pentads 11 and 13 which are equivalent to 51-55 days and 61-65 days at 850hPa and 700-hPa respectively. The time lags obtained for the predicted onset for this study agrees with the results obtained by Kerandi (2008) for Dagoretti station for both surface and 700hPa for the MAM season as shown in Equation 13 and 14.

$$POR_{850hPa} = X+11 \dots \dots \dots (13)$$

$$POR_{700hPa} = X+13 \dots \dots \dots (14)$$

In equations 13 and 14, *POR* is the Predicted Onset of Rainfall and X is the pentad date obtained when $\theta_e > 0$.

Over Kisumu time lags of pentads 8 and 10 were obtained for MAM and OND respectively while Marsabit obtained a time lag of pentad 15 for MAM season at 700-hPa level. With knowledge on the time lags at local level (station level) the prediction of onset can be done when the equivalent potential temperature anomaly is positive for 2 or 3 pentads while cessation can be done when there is maximum separation between equivalent potential temperature and saturation equivalent potential temperature.

Table 4: Predicted rainfall onset in pentads obtained using Actual Rainfall Onset and equivalent potential temperature anomaly ($\theta_e > 0$) in Pentads during MAM season, at 850-hPa for Dagoretti station

Years	Actual Rainfall Onset in Pentads	$\theta_e > 0$ (X)	Difference (Actual rainfall onset in pentads minus $\theta_e > 0$)	Predicted onset of rainfall in Pentads (X+11(mean))
1989	16	7	9	18
1992	18	3	15	14
1994	21	1	20	12
1995	8	1	7	12
1998	20	9	11	20
1999	14	1	13	12
2001	13	1	12	12
2003	22	8	14	19
2004	14	1	13	12
2005	16	2	14	13
2006	11	2	9	13
2008	14	3	11	14
2012	21	2	19	13
2013	16	6	10	17
2014	14	1	13	12
2015	18	16	2	27
2016	13	12	1	23
2018	12	10	2	21
Mean (time lag)			11	

Table 5: Predicted rainfall onset in pentads using Actual Rainfall Onset and equivalent potential temperature anomaly ($\theta'_e > 0$) in Pentads during MAM season, at 700-hPa for Dagoretti station

Years	Actual Rainfall Onset in Pentads	$\theta'_e > 0$ (X)	Difference (Actual rainfall onset in pentads minus $\theta'_e > 0$)	Predicted Onset in Pentads (X+13(mean))
1989	16	4	12	17
1992	18	3	15	16
1994	21	1	20	14
1995	8	1	7	14
1997	18	1	17	14
1998	20	8	12	21
1999	14	2	12	15
2001	13	5	8	18
2002	12	3	9	16
2004	14	1	13	14
2005	16	2	14	15
2006	11	3	8	16
2008	14	3	11	16
2009	26	4	22	17
2010	17	1	16	14
2012	21	2	19	15
2014	14	4	10	17
2015	18	2	16	15
2016	13	2	11	15
2018	12	13	-1	26
Mean (average)			13	

Table 6: Predicted rainfall onset in pentads using Actual Rainfall Onset and equivalent potential temperature anomaly ($\theta_e > 0$) in pentads during MAM season, at 850-hPa for Kisumu station

Years	Actual Rainfall Onset in Pentads	$\theta_e > 0$ (X)	Difference (Actual rainfall onset in pentads minus $\theta_e > 0$)	Predicted Onset in Pentads (X+11(mean))
1989	14	6	8	17
1991	16	10	6	21
1992	17	4	13	15
1993	20	10	10	21
1995	18	6	12	17
1997	16	4	12	15
1998	18	4	14	15
1999	11	1	10	12
2000	21	1	20	12
2001	17	9	8	20
2003	15	8	7	19
2004	16	2	14	13
2005	14	2	12	13
2006	11	2	9	13
2007	13	4	9	15
2010	8	2	6	13
2011	21	1	20	12
2012	17	2	15	13
2013	14	1	13	12
2014	13	4	9	15
2015	15	11	4	22
2016	17	1	16	12
2017	20	5	15	16
Mean(average)			11	

Table 7: Determination of Predicted rainfall onset in pentads using Actual Rainfall Onset and $\theta'_e > 0$ in pentads during MAM season, at 700-hPa for Kisumu station

Years	Actual Rainfall onset in Pentads	$\theta'_e > 0$ (X)	Difference (Actual rainfall onset in pentads minus $\theta'_e > 0$)	Predicted Onset in Pentads (X+8(mean))
1989	22	6	16	14
1990	24	6	18	14
1991	14	11	3	19
1992	8	3	5	11
1994	16	1	15	9
1995	7	1	6	9
1996	7	10	-3	18
1997	14	4	10	12
1999	10	2	8	10
2000	10	1	9	9
2001	7	8	-1	16
2002	8	1	7	9
2003	21	4	17	12
2004	9	2	7	10
2006	8	3	5	11
2007	20	3	17	11
2008	8	3	5	11
2010	8	1	7	9
2011	7	2	5	10
2012	7	2	5	10
2013	8	1	7	9
2014	9	4	5	12
2015	7	2	5	10
2017	10	5	5	13
Mean (average)			8	

Table 8: Determination of Predicted rainfall onset in pentads using Actual Rainfall Onset and $\theta_e > 0$ in pentads during MAM season, at 700-hPa for Marsabit station

Years	Actual Rainfall Onset in Pentads	$\theta_e > 0$ (X)	Difference (Actual rainfall onset in pentads minus $\theta_e > 0$)	Predicted Onset in Pentads (X+15(mean))
1989	21	4	17	19
1990	19	2	17	17
1991	22	3	19	18
1992	19	5	14	20
1993	18	4	14	19
1994	18	3	15	18
1995	22	12	10	27
1997	19	5	14	20
1998	19	9	10	24
1999	21	3	18	18
2000	22	2	20	17
2001	19	3	16	18
2002	19	6	13	21
2004	19	2	17	17
2006	21	5	16	20
2009	19	4	15	19
2011	18	4	14	19
2012	20	4	16	19
2013	19	3	16	18
2014	22	2	20	17
2016	20	6	14	21
Mean (average)			15	

Table 9: Times lags in Pentads for MAM and OND season at 850hPa and 700hPa level for the stations used

MAM	850hPa		700hPa	
	Onset in pentads	Cessation in pentads	Onset in pentads	Cessation in pentads
Dagoretti	11	14	13	12
Kisumu	11	19	8	19
Marsabit	12	13	15	7
Moyale	12	15	13	5
Nanyuki	13	15	11	16
Narok	8	10	15	11
Voi	9	12	11	12
Wajir	7	12	12	10
OND				
Dagoretti	15	2	22	2
Kisumu	7	5	10	9
Marsabit	21	4	13	4
Moyale	9	NaN	17	11
Nanyuki	11	11	16	9
Narok	19	6	20	3
Voi	14	2	21	5
Wajir	10	0	19	7

***NaN implies missing, resulting from the criteria not met.**

Figures 13-17 are the time series plots demonstrating the year to year variability between the actual and predicted onset and the actual and predicted cessation. Most stations have shown less uniformity in the series except for some years. The time series for the Narok station (Figure 13) at 700 hPa level during the MAM season, shows consistency in the series of actual and predicted onset between the years 1999-2004 with the rest of the years showing inconsistency. Same observation between the actual and predicted cessation during the years 2007-2013 was reported with same scenario for other time series (Figure 14-16). Figure 17 demonstrate the time series for Moyale, a perfect uniform time series for actual and predicted cessation is observed.

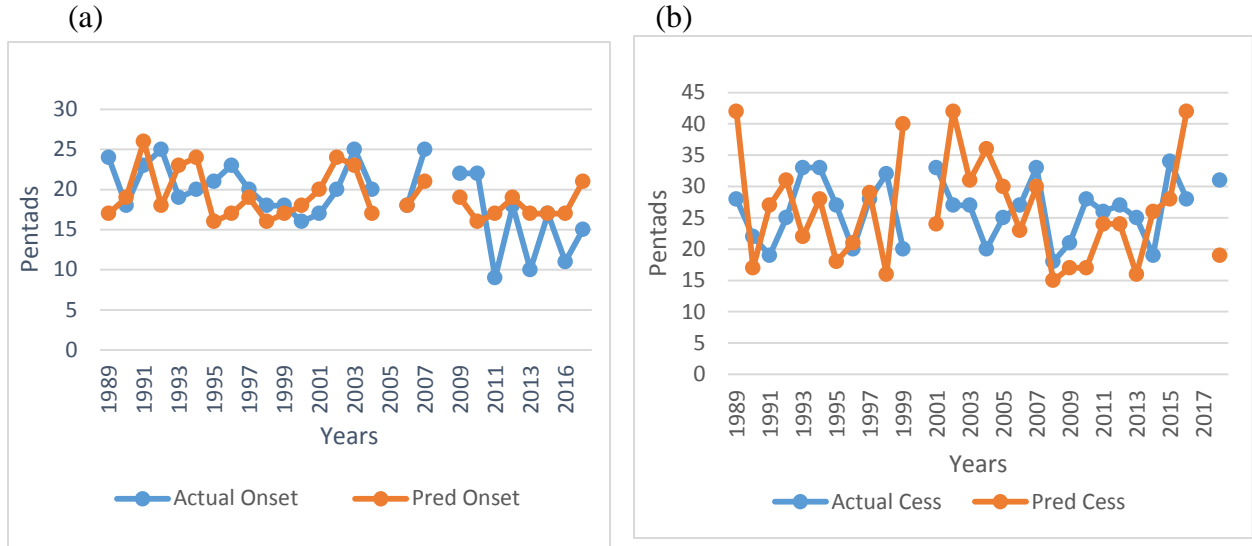
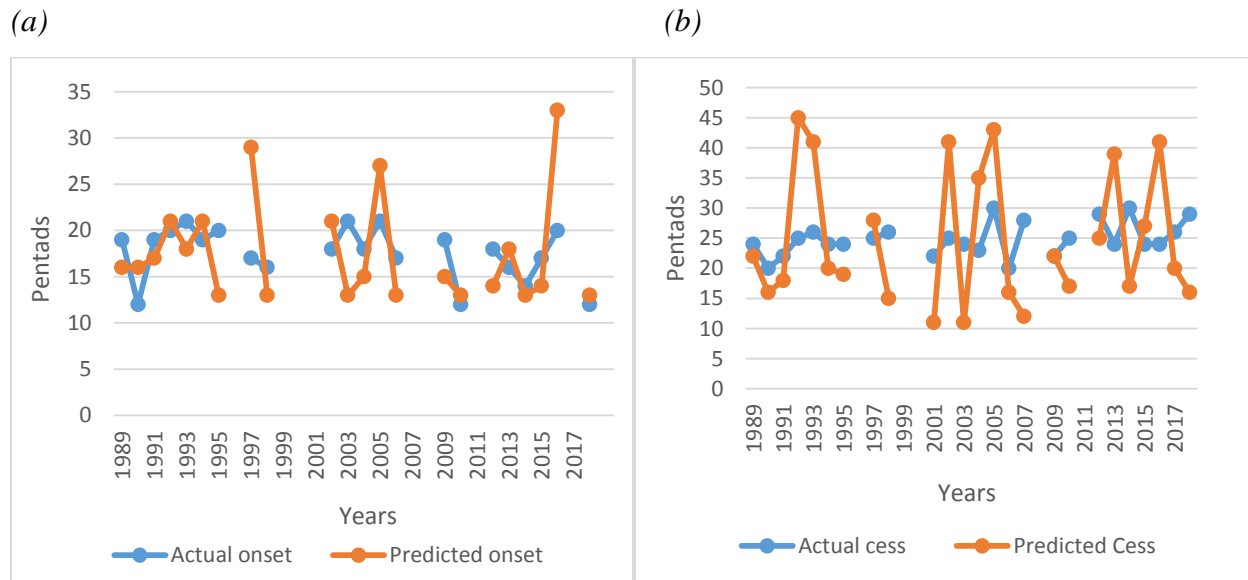


Figure 13: Time series for actual and predicted rainfall onset (a) and cessation (b) for Narok station using equivalent and saturated equivalent potential temperature anomalies at 700hPa during the MAM season



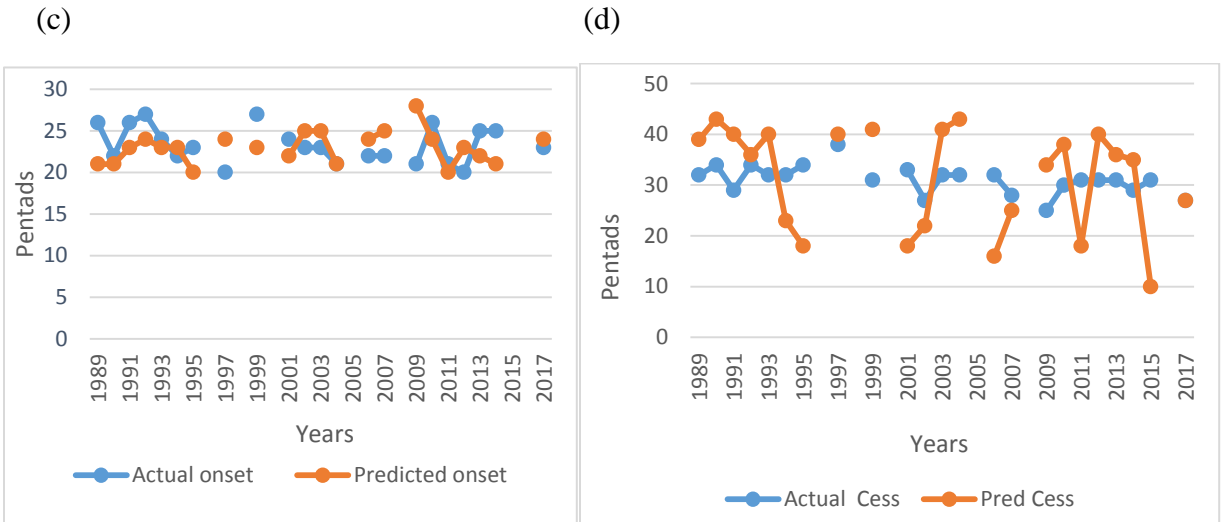
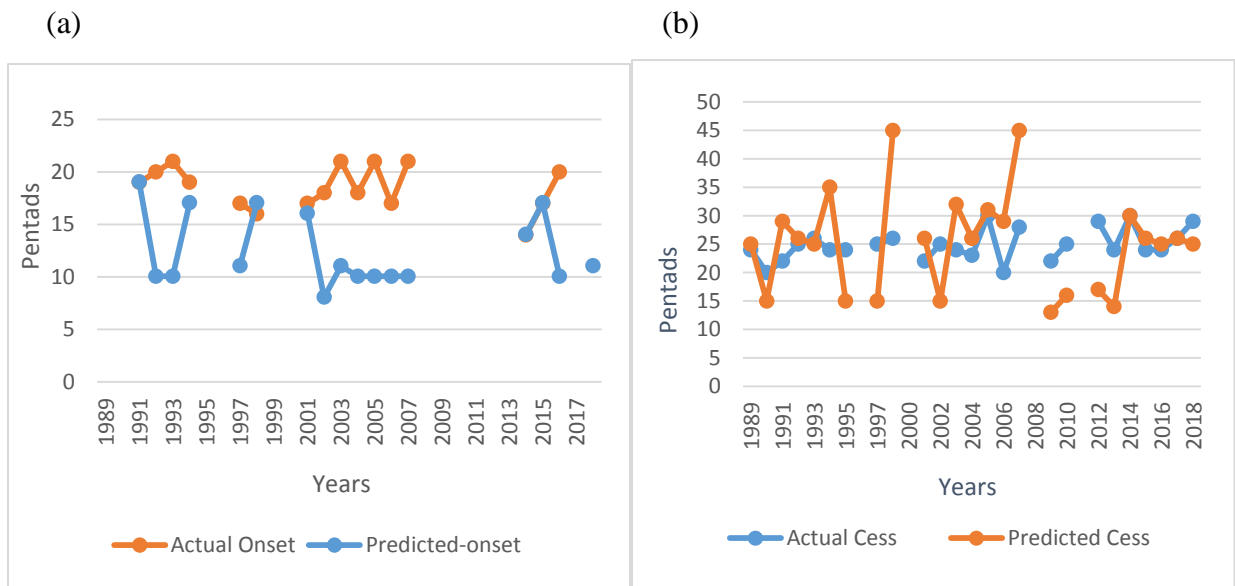


Figure 14: Time series for actual and predicted rainfall onset(a) and cessation (b) during MAM season and actual and predicted rainfall onset(c) and cessation (d) for Wajir during OND season: using equivalent and saturated equivalent potential temperature anomalies 700hPa



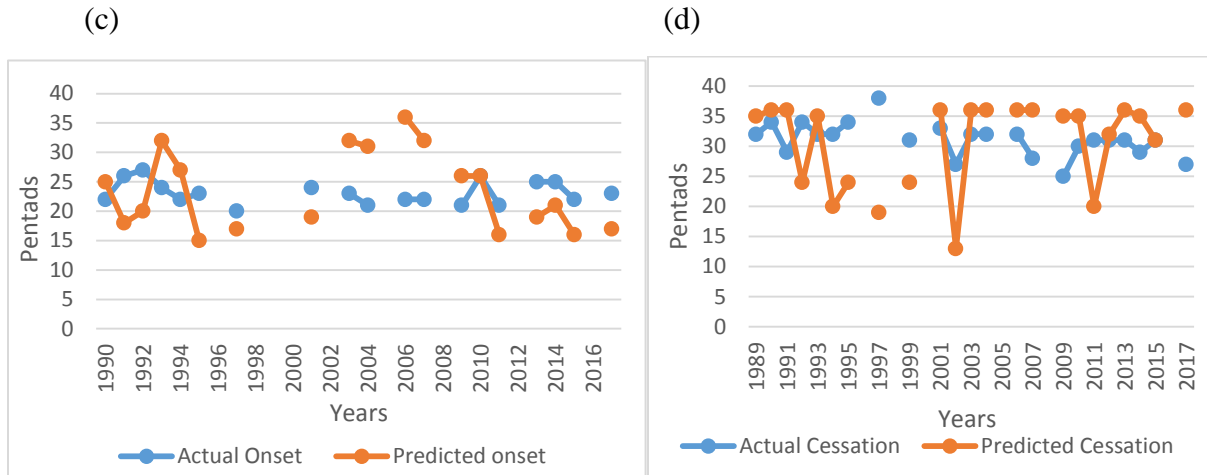


Figure 15: Time series for actual and predicted rainfall onset(a) and cessation (b) during MAM season and actual and predicted rainfall onset(c) and cessation (d) for Wajir during OND season: using equivalent and saturated equivalent potential temperature anomalies 850 hPa

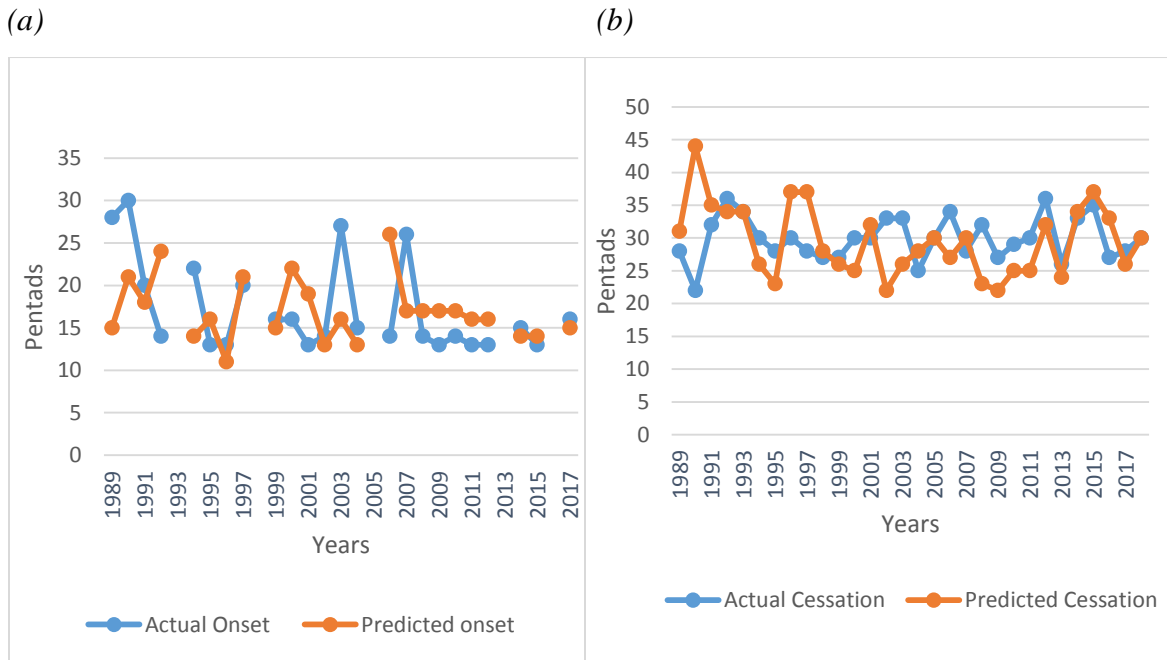


Figure 16: Time series for actual and predicted rainfall onset (a) and cessation (b) for Kisumu using equivalent and saturated equivalent potential temperature anomalies at 700hPa OND season

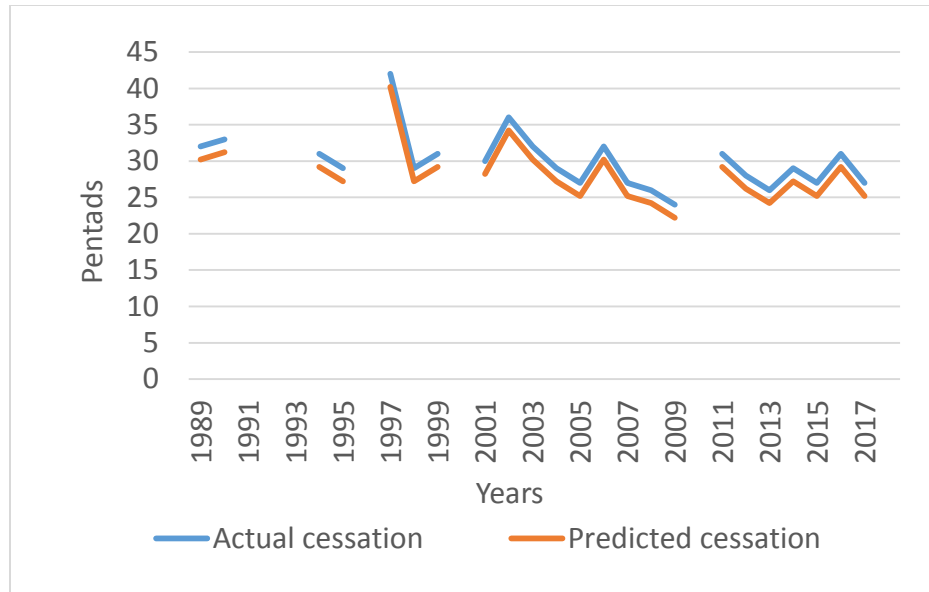


Figure 17: Time series for actual and predicted cessation for Moyale using equivalent and saturated equivalent potential temperature anomalies at 850 hPa OND season

4.3.1 Correlation analysis

Table 10 demonstrates the relationship between the actual and predicted onset, and the actual and predicted cessation. The values in bold shows negative or positive correlation coefficient (cc) with significance at 95% confidence level. The correlation coefficient between actual and predicted onset, and the actual and predicted cessation was insignificant for most stations. Kisumu, Moyale, Voi and Wajir recorded some significant correlation. Kisumu for instance recorded significant relationship with a correlation coefficient of 0.424 (-0.523) between actual and predicted onset (cessation) at 850 hPa level during the October-November-December season. Moyale recorded a correlation coefficient (CC) of 0.401 (-0.372) between the actual and predicted cessation for 850 hPa (700 hPa) level while a CC of -0.375 (1) between the actual and predicted onset (cessation) during the OND season at 850 hPa.

It is observed that most of the stations during OND season have shown significant relationship but with variability. This implies that significance in the correlation coefficient can be observed between the actual and predicted onset for 700 hPa or 850 hPa or both while the actual and predicted cessation for the season depicts insignificance in the correlation coefficient.

The results also show that OND season has better association as compared to MAM season. This is because the large-scale systems (regional and global teleconnections) prevail during this

season (Owiti *et al.*, 2008) leading to incursions of moisture since the atmosphere is not in isolated state.

The 850 hPa level shows a better association as compared to the 700 hPa level. This is attributed to more presence of moisture at the low levels and it decreases as the level increases (Holloway and Neelin, 2009).

Table 10: Pearson Correlation Coefficient demonstrating the relationship between Actual and Predicted onset, and Actual and Predicted Cessation for MAM and OND obtained using equivalent potential temperature and saturation equivalent potential temperature at 700hPa and 850hPa levels. The values in bold are the significant values at 5% significant level.

Station	Actual vs Predicted onset for MAM		Actual vs Predicted cessation for MAM		Actual vs Predicted onset for OND		Actual vs Predicted cessation for OND	
	700hPa	850hPa	700hPa	850hPa	700hPa	850hPa	700hPa	850hPa
Kisumu	0.247	0.193	-0.049	0.092	0.077	0.424	0.240	-0.523
Narok	0.284	0.211	-0.03	0.057	0.315	0.170	0.219	0.131
Dagoretti	-0.066	0.208	-0.266	-0.127	-0.08	0.349	0.119	-0.087
Nanyuki	-0.18	-0.158	-	0.065	-0.246	0.195	-0.047	-0.228
Wajir	0.379	-0.372	0.188	0.248	-0.113	-0.155	0.143	-0.518
Marsabit	0.092	0.285	0.004	-0.216	-0.002	-0.287	0.071	-0.334
Moyale	-0.304	-0.090	-0.372	0.401	0.180	-0.376	-0.068	1
Voi	0.120	0.183	0.347	0.233	0.125	-0.306	0.211	-0.003

CHAPTER FIVE

5.0 CONCLUSIONS AND RECOMMENDATIONS

This chapter highlights a summary of the results obtained from the various methods used to accomplish the objective of the study. Moreover, it provides the conclusions and the recommendations made.

5.1 CONCLUSIONS

The overall objective of this research was to assess the potential of predicting onset and cessation dates of seasonal rainfall in Kenya using tropospheric moisture accumulation. Dates of the start and cessation of rainfall dates were determined using the first PCA score (PC1). Time series plots was used to determine the moisture build up and withdrawal dates, and linking the start and end of rainfall dates to the tropospheric moisture accumulation so as to see the possibility of predicting seasonal rainfall prior to the start and to the end by using time lags developed. The datasets used in the study are daily rainfall data obtained from CHIRPS: daily Temperature and relative humidity obtained from ERA5 at 850 hPa and 700 hPa, spanning for a period of 1989-2018. The CHIRPS data were extracted for 1 grid, 4 grids and 16 grids then subjected to PCA in order to identify the score to use. The cumulative PC1 score was used to determine the yearly rainfall start and end dates.

The minimum (maximum) point of the accumulated PC 1 scores represented the onset (cessation) of rainfall. Mean onset ranged from 15th March to 08th April while the cessation ranged from 20th April to 29th May during the MAM season. The OND season had a mean onset (cessation) of rains that ranged from 23rd September to 11th November (28th November to 27th December). Stations in the western region recorded an early mean onset during both long and short rain seasons with an easterly progression. An early mean onset was also observed at the coastal region during the OND season. This is attributed to the large-scale systems and coupled ocean atmospheric systems, which are active during this season pushing the warm moist air masses to the land. Longer rainy duration was observed over the western region while the shorter rainy season was observed at the north eastern region.

Time series plots were used to identify the dates of onset and withdrawal of moisture accumulation. The mean start (end) dates of moisture build up ranged from pentads 3 to 6 (pentads 11 to 15) during the MAM season and pentads 4 to 7 (pentads 14 to 24) during the

OND at the 700 hPa level. Using the data at 850 hPa level, the mean start (end) dates of moisture ranged from pentads 4 to 8 (pentads 9 to 17) during the MAM season while during the OND season the mean start and end dates ranged from pentads 41 to 49 and pentads 53 to 69 respectively.

The time lags are the link between the start and end dates of rainfall, and the onset and withdrawal dates of moisture accumulation. It ranged from pentad number 7 to 15 for the onset and pentad number 10 to 19 for the cessation using the data at 850 hPa level while at the 700 hPa level, the onset (cessation) of moisture ranged from 8 to 15 (5 to 19) pentads during the MAM season. Conversely, the OND season recorded 7 to 15 (2 to 11) pentads for the onset (cessation) dates of moisture build up at the 850 hPa whereas 10 to 22 and 2 to 11 pentads were obtained for the onset and cessation of moisture build up respectively at the 700 hPa. There were discrepancies during some years between the results of this study and that of Kerandi (2008). However, the results obtained for Dagoretti station during the MAM season were in agreement with time lags of 11 and 13 pentads for 850 hPa and 700 hPa respectively.

The study has demonstrated that the forecast for the start of the rainy season can be done with a lead time of 2 to 3 pentads using equivalent potential temperature anomaly while the forecast for the end of the rainy season can be done using the difference between the equivalent potential temperature and the saturation equivalent potential temperature anomalies at 850 hPa and 700 hPa.

The results of the study have shown to some degree the potential of utilizing tropospheric moisture variables in predicting start and end dates of rainfall over the study domain.

5.2 RECOMMENDATIONS

This section presents important recommendations drawn from the results of the study to various stakeholders.

5.2.1 Recommendation to Climate Services Providers and Policy Makers

The National Meteorological and Hydrological Services (NMHS) is encouraged to incorporate tropospheric moisture variables in the prediction of start and end dates of rainfall in order to give a timely and reliable forecast. This will benefit the end users as losses and risks related to forecast uncertainties are minimized. NMHS are also encouraged to improve the upper air observations

so that similar studies as well as operational utilization of the onset and cessation forecasting methodology presented in this research may be actualized.

An establishment of regular and efficient communication network is highly encouraged for timely dissemination of research findings to its potential users. Moreover, community-based education be undertaken in order to create in depth understanding of the results. This will ensure timely integration of the findings for planning purposes by the potential users.

5.2.2 Recommendations to Scientists and Climate Research Institutions

The results obtained in this study on the linkage between rainfall onset and cessation; the commencement and withdrawal dates of moisture build up, portrayed variability. Further study is recommended to investigate the distinct variability observed using the in situ data to support these results. Since some stations during some years showed significant association while others showed insignificant relationship. Moreover, further studies on the linkage with the synoptic systems (for example winds) for both MAM and OND season are highly recommended.

5.2.3 Recommendation to Users of Climate Information

The findings of this study can be used by the agricultural sector to advise farmers on when and what to plant in order to avoid crop failure associated with late start, early end and the shorter rain season. Pastoralists as well are encouraged to actively use the results in order to reduce climate related loses of their livestock. The energy and water sector are advice to use the results for planning purposes.

References

- Albergel, C., Munier, S., Bocher, A., Bonan, B., Zheng, Y., Draper, C., Leroux, D. J. and Calvet, J. (2018). *LDAS-Monde Sequential Assimilation of Satellite Derived Observations Applied to the Contiguous US : An ERA-5 Driven Reanalysis of the Land Surface Variables*. 1–24. <https://doi.org/10.3390/rs10101627>
- Alusa, A. L. and Mushi, M. T. (1974). A study of the onset, duration and cessation of the rains in East Africa. *Preprints, International Tropical Meteorology Meeting, Nairobi, 21 Jan–7 Feb 1974*, 133–140.
- Asnani, G. C. (1993). *Tropical meteorology*. Asnani, Indian Inst. of Tropical Meteorology.
- Bahaga, T. K., Mengistu Tsidu, G., Kucharski, F. and Diro, G. T. (2015). Potential predictability of the sea-surface temperature forced equatorial east african short rains interannual variability in the 20th century. *Quarterly Journal of the Royal Meteorological Society*, *141*(686), 16–26. <https://doi.org/10.1002/qj.2338>
- Bärring, L. (1988). Regionalization of daily rainfall in Kenya by means of common factor analysis. *Journal of Climatology*, *8*(4), 371–389.
- Barron, J., Gichuki, F. and Hatibu, N. (2003). Dry spell analysis and maize yields for two semi-arid locations in East Africa. *117*, 23–37. [https://doi.org/10.1016/S0168-1923\(03\)00037-6](https://doi.org/10.1016/S0168-1923(03)00037-6)
- Bosire, N. E . (2019). Simulating impacts of climate change on sorghum production in the semi-arid environment of Katumani in Machakos County. *PhD thesis, Department of Meteorology, University of Nairobi*
- Camberlin, P. and Okoola, R. E. (2003). The onset and cessation of the ““ long rains ”” in eastern Africa and their interannual variability. *Theoretical and Applied Climatology*, *54*(1–2), 43–54. <https://doi.org/10.1007/s00704-002-0721-5>
- Camberlin, P. and Diop, M. (2003). Application of daily rainfall principal component analysis to the assessment of the rainy season characteristics in Senegal. *Climate Research*, *23*(2), 159–169.
- Camberlin, P. and Philippon, N. (2002). The East African March-May rainy season: Associated atmospheric dynamics and predictability over the 1968-97 period. *Journal of Climate*,

15(9), 1002–1019. [https://doi.org/10.1175/1520-0442\(2002\)015<1002:TEAMMR>2.0.CO;2](https://doi.org/10.1175/1520-0442(2002)015<1002:TEAMMR>2.0.CO;2)

- Camberlin, P, Moron, V., Okoola, R., Philippon, N. and Gitau, W. (2009). Components of rainy seasons' variability in Equatorial East Africa: Onset, cessation, rainfall frequency and intensity. *Theoretical and Applied Climatology*, 98(3–4), 237–249. <https://doi.org/10.1007/s00704-009-0113-1>
- Dinku, T., Funk, C., Peterson, P., Maidment, R., Tadesse, T., Gadain, H. and Ceccato, P. (2018). Validation of the CHIRPS satellite rainfall estimates over eastern Africa. *Quarterly Journal of the Royal Meteorological Society*, 144(November 2017), 292–312. <https://doi.org/10.1002/qj.3244>
- Dunning, C. M., Black, E. C. L. and Allan, R. P. (2016). The onset and cessation of seasonal rainfall over Africa. *Journal of Geophysical Research*, 121(19), 11405–11424. <https://doi.org/10.1002/2016JD025428>
- Endris, H. S., Lennard, C., Hewitson, B., Dosio, A., Nikulin, G. and Artan, G. A. (2019). Future changes in rainfall associated with ENSO, IOD and changes in the mean state over Eastern Africa. *Climate Dynamics*, 52(3–4), 2029–2053. <https://doi.org/10.1007/s00382-018-4239-7>
- Gitau, W. (2011). Diagnosis and predictability of intraseasonal characteristics of wet and dry spells over equatorial east Africa. *PhD thesis, Department of Meteorology, University of Nairobi.*
- Holloway, C. E. and Neelin, D. J. (2009). Moisture vertical structure, column water vapor, and tropical deep convection. *Journal of the Atmospheric Sciences*, 66(6), 1665–1683. <https://doi.org/10.1175/2008JAS2806.1>
- Indeje.M. (2000). Prediction and numerical simulation of the regional climate of Equatorial Eastern Africa [North Carolina State University]. <https://repository.lib.ncsu.edu/bitstream/handle/1840.16/4840/etd.pdf?sequence=1&isAllowed=y>
- Indeje, M., Semazzi, F. H. M., Xie, L. and Ogallo, L. J. (2001). Mechanistic model simulations of the East African climate using NCAR regional climate model: Influence of large-scale orography on the Turkana low-level jet. *Journal of Climate*, 14(12), 2710–2724.

[https://doi.org/10.1175/1520-0442\(2001\)014<2710:MMSOTE>2.0.CO;2](https://doi.org/10.1175/1520-0442(2001)014<2710:MMSOTE>2.0.CO;2)

- Jolliffe, I. T. and Sarria-dodd, D. E. (1994). Early detection of the start of the wet season in tropical climates. *International Journal of Climatology*, 14(1), 71–76.
- Kerandi, N. M., (2008). Seasonal Rainfall Prediction in Kenya Using Empirical Methods. *Journal of Kenya Meteorological Society*, 2(2)(11), 114–124.
- Kipkogei, O., Mwanthi, A. M., Mwesigwa, J. B., Atheru, Z. K. K., Wanzala, M. A. and Artan, G. (2017). Improved seasonal prediction of rainfall over East Africa for application in agriculture: Statistical downscaling of CFSv2 and GFDL-FLOR. *Journal of Applied Meteorology and Climatology*, 56(12), 3229–3243. <https://doi.org/10.1175/JAMC-D-16-0365.1>
- Koech, E. (2014). Systems Associated With Wet Spells Over Kenya During the Usually Dry December-February Season. *MSc thesis, Department of Meteorology, University of Nairobi*
- Liebmann, B., Bladé, I., Kiladis, G. N., Carvalho, L. M. V, B. Senay, G., Allured, D., Leroux, S. and Funk, C. (2012). Seasonality of African precipitation from 1996 to 2009. *Journal of Climate*, 25(12), 4304–4322.
- Macleod, D. (2018). Seasonal predictability of onset and cessation of the east African rains. *Weather and Climate Extremes*, 21(June), 27–35. <https://doi.org/10.1016/j.wace.2018.05.003>
- Marengo, J. A., Liebmann, B., Kousky, V. E., Filizola, N. P. and Wainer, I. C. (2001). Onset and end of the rainy season in the Brazilian Amazon Basin. *Journal of Climate*, 14(5), 833–852. [https://doi.org/10.1175/1520-0442\(2001\)014<0833:OAEOTR>2.0.CO;2](https://doi.org/10.1175/1520-0442(2001)014<0833:OAEOTR>2.0.CO;2)
- Mhita, M. S. and Nassib, I. R. (1987). The onset and end of rain in Tanzania. *Proc 1st Tech Conf Meteorol Res East South Afr*, 101–115.
- Micheau Boyard, J., Camberlin, P., Philippon, N. and Moron, V. (2013). Regional-Scale Rainy Season Onset Detection: A New Approach Based on Multivariate Analysis. *Journal of Climate*, 26(22), 8916–8928. <https://doi.org/10.1175/JCLI-D-12-00730.1>
- Mugalavai, E. M., Kipkorir, E. C., Raes, D. and Rao, M. S. (2008). Analysis of rainfall onset, cessation and length of growing season for western Kenya. *Agricultural and Forest*

- Meteorology*, 148(6–7), 1123–1135. <https://doi.org/10.1016/j.agrformet.2008.02.013>
- Mukabana, J. R. and Piekle, R. A. (1996). Investigating the Influence of Synoptic-Scale Monsoonal Winds and Mesoscale Circulations on Diurnal Weather Patterns over Kenya Using a Mesoscale Numerical Model. *Monthly Weather Review*, 124(2), 224–244. [https://doi.org/10.1175/1520-0493\(1996\)124<0224:ITIOSS>2.0.CO;2](https://doi.org/10.1175/1520-0493(1996)124<0224:ITIOSS>2.0.CO;2)
- Mutai, C. C. (2000). Diagnosis and predictability of East African rainfall on intraseasonal to interannual timescales. *PhD thesis, Department of Meteorology, University of Nairobi*
- Mutai, C. C. and Ward, M. N. (2000). East African Rainfall and the Tropical Circulation/Convection on Intraseasonal to Interannual Timescales. *Journal of Climate*, 13(22), 3915–3939. [https://doi.org/10.1175/1520-0442\(2000\)013<3915:EARATT>2.0.CO;2](https://doi.org/10.1175/1520-0442(2000)013<3915:EARATT>2.0.CO;2)
- Mutemi, J. N. (2003). Climate anomalies over eastern Africa associated with various ENSO evolution phases. *PhD thesis, Department of Meteorology, University of Nairobi, Kenya.*
- Mwanthi, A. M. (2015). Investigating Linkages Between the Subtropical Indian Ocean Dipole Mode and East Africa Rainfall During October To December. *MSc Dissertation, Department of Meteorology, University of Nairobi*
- Ngetich, K. F., Mucheru-muna, M., Mugwe, J. N., Shisanya, C. A., Diels, J. and Mugendi, D. N. (2014). Agricultural and Forest Meteorology Length of growing season , rainfall temporal distribution , onset and cessation dates in the Kenyan highlands. *Agricultural and Forest Meteorology*, 188, 24–32. <https://doi.org/10.1016/j.agrformet.2013.12.011>
- Nicholson, S. E. (2017). Climate and climatic variability of rainfall over eastern Africa. *Reviews of Geophysics*, 55(3), 590–635. <https://doi.org/10.1002/2016RG000544>
- Nicholson, S. (2016). The Turkana low-level jet: Mean climatology and association with regional aridity. *International Journal of Climatology*, 36(6), 2598–2614. <https://doi.org/10.1002/joc.4515>
- Njau, L. N. (2006). Diagnostics and predictability of East African rainfall with tropospheric circulation parameters. *PhD thesis, Department of Meteorology, University of Nairobi*
- Nyakwada, W. (2009). Predictability of East African seasonal rainfall with sea surface

- temperature gradient modes. *PhD thesis, Department of Meteorology, University of Nairobi*
- Odekunle, T. O. (2006). *Determining rainy season onset and retreat over Nigeria from precipitation amount and number of rainy days.* 201, 193–201. <https://doi.org/10.1007/s00704-005-0166-8>
- Oettli, P. and Camberlin, P. (2005). Influence of topography on monthly rainfall distribution over East Africa. *Climate Research*, 28(3), 199–212. <https://doi.org/10.3354/cr028199>
- Ogallo, L. J. (1982). Quasi-periodic patterns in the East African rainfall records. *Kenya J. Sci. and Technology*, 3, 43-54
- Okeyo, A. E. (1986). The Impact of Lake Victoria on the Convective Activities over the Kenya Highlands. *Journal of the Meteorological Society of Japan. Ser. II*, 64A, 689–695. https://doi.org/10.2151/jmsj1965.64a.0_689
- Okoola, R. E. (1998). Spatial evolutions of the active convective patterns across the equatorial eastern Africa region during Northern Hemisphere spring season using outgoing longwave radiation records. *Met. and Atm. Physics*, 66(1–2), 51–63.
- Okoola, R. E. (1999). A diagnostic study of the eastern Africa monsoon circulation during the Northern Hemisphere spring season. *Int. J. of Climatol.*, 19(2), 143–168. [https://doi.org/10.1002/\(SICI\)1097-0088\(199902\)19:2<143::AID-JOC342>3.0.CO;2-U](https://doi.org/10.1002/(SICI)1097-0088(199902)19:2<143::AID-JOC342>3.0.CO;2-U)
- Omeny, P. A., Ogallo, L., Okoola, R.E, Hendon, H. and WHEELER, M. (2008). East African rainfall variability associated with the Madden-Julian Oscillation. *Journal of Kenya Meteorological Society Volume*, 2(2).
- Omondi, M. H. (2015). Assessment of temperature and precipitation extremes over Kenya using the Coordinated Regional Downscaling Experiment model outputs. *MSc. Dissertation, Department of Meteorology, University of Nairobi*
- Omotosho, J. B. (1990). Onset of thunderstorms and precipitation over Northern Nigeria. *International Journal of Climatology*, 10(8), 849–860. <https://doi.org/10.1002/joc.3370100807>
- Omotosho, J. B., Balogun, A. A. and Ogunjobi, K. (2000). Predicting monthly and seasonal rainfall ,onset and cessation of the rainy season in West Africa using only surface data.

International Journal of Climatology, 20(8), 865–880. [https://doi.org/10.1002/1097-0088\(20000630\)20:8<865::AID-JOC505>3.0.CO;2-R](https://doi.org/10.1002/1097-0088(20000630)20:8<865::AID-JOC505>3.0.CO;2-R), 865–880

- Otieno, G., Mutemi, J. N., Opijah, F. J., Ogallo, L. A. and Omondi, M. H. (2020). The Sensitivity of Rainfall Characteristics to Cumulus Parameterization Schemes from a WRF Model. Part I: A Case Study Over East Africa During Wet Years. *Pure and Applied Geophysics*, 177(2), 1095–1110. <https://doi.org/10.1007/s00024-019-02293-2>
- Owiti, O. Z. (2005). Use of the Indian Ocean Dipole indices as predictor east African rainfall anomalies. *MSc Thesis, Department Of Meteorology, University of Nairobi*.
- Owiti, Z., Ogallo, L. A. and Mutemi, J. (2008). Linkages between the Indian Ocean Dipole and East African seasonal rainfall anomalies. *Journal of Kenya Meteorological Society Volume*, 2(1).
- Pohl, B. and Camberlin, P. (2006). Influence of the Madden–Julian oscillation on East African rainfall. I: Intraseasonal variability and regional dependency. *Quarterly Journal of the Royal Meteorological Society: A Journal of the Atmospheric Sciences, Applied Meteorology and Physical Oceanography*, 132(621), 2521–2539.
- Recha, C. W., Makokha, G. L., Traore, P. S., Shisanya, C., Lodoun, T. and Sako, A. (2012). Determination of seasonal rainfall variability, onset and cessation in semi-arid Tharaka district, Kenya. *Theoretical and Applied Climatology*, 108(3–4), 479–494.
- Semazzi, F. H. M., Burns, B., Lin, N.-H. and Schemm, J.-K. (1996). A GCM Study of the Teleconnections between the Continental Climate of Africa and Global Sea Surface Temperature Anomalies. *Journal of Climate*, 9(10), 2480–2497. [https://doi.org/10.1175/1520-0442\(1996\)009<2480:AGSOTT>2.0.CO;2](https://doi.org/10.1175/1520-0442(1996)009<2480:AGSOTT>2.0.CO;2)
- Sivakumar, M. V. (1988). Predicting rainy season potential from the onset of rains in Southern Sahelian and Sudanian climatic zones of West Africa. *Agricultural and Forest Meteorology*, 42 (1988) 295-305, 42, 295–305.
- Stewart, J. I. and Hash, C. T. (1982). Impact of weather analysis on agricultural production and planning decisions for the semiarid areas of Kenya. *Journal of Applied Meteorology*, 21(4), 477–494.
- Urraca, R., Huld, T., Gracia-amillo, A., Martinez-de-pison, F. J., Kaspar, F. and Sanz-garcia, A.

(2018). Evaluation of global horizontal irradiance estimates from ERA5 and COSMO-REA6 reanalyses using ground and satellite-based data. *Solar Energy*, 164(February), 339–354. <https://doi.org/10.1016/j.solener.2018.02.059>

Zhang, X., Liang, S., Wang, G., Yao, Y., Jiang, B. and Cheng, J. (2016). Evaluation of the reanalysis surface incident shortwave radiation products from NCEP, ECMWF, GSFC, and JMA using satellite and surface observations. *Remote Sensing*, 8(3), 225.